processes

MDPI

Article

Decarbonizing Arctic Mining Operations with Wind-Hydrogen Systems: Case Study of Raglan Mine

Hugo Azin, Baby-Jean Robert Mungyeko Bisulandu, Adrian Ilinca * and Daniel R. Rousse

Mechanical Engineering, T3E Research Group, École de Technologie Supérieure (ÉTS), Montréal, QC H3C 1K3, Canada; hugo.azin.1@ens.etsmtl.ca (H.A.); baby-jeanrobert.mungyekobisulandu@etsmtl.ca (B.-J.R.M.B.); daniel.rousse@etsmtl.ca (D.R.R.)
* Correspondence: adrian.ilinca@etsmtl.ca

Abstract

This study evaluates the techno-economic feasibility of integrating wind power with hydrogen-based storage to decarbonize the Raglan Mine in northern Canada. Using HOMER simulations with real 2021 operational data, six progressive scenarios were modeled, ranging from partial substitution of diesel generators to complete site-wide electrification, including heating, transport, and mining equipment. Results show that complete decarbonization (Scenario 6) is technically achievable and could avoid up to 143,000 tCO_2eq annually (~2.15 Mt over 15 years), but remains economically prohibitive under current technology costs. In contrast, Scenario 2 Case 2, which combines solid oxide fuel cells with thermal charge controllers, emerges as the most viable near-term pathway, avoiding ~61,000 tCO_2eq annually (~0.91 Mt over 15 years) while achieving improved return on investment. A qualitative multi-criteria framework highlights this configuration as the best trade-off between technical feasibility, environmental performance, and economic viability. At the same time, complete decarbonization remains a longer-term target contingent on cost reductions and policy support. Overall, the findings provide clear evidence that hydrogen storage, when coupled with wind power, can deliver substantial and measurable decarbonization benefits for Arctic mining operations.

Keywords: modeling; decarbonization; hydrogen storage; renewable energies; PEM; ROI

Academic Editors: Mohammed Jama, Addy Wahyudie and Michael C. Georgiadis

Received: 20 August 2025
Revised: 6 October 2025
Accepted: 6 October 2025
Published: 9 October 2025

Citation: Azin, H.; Mungyeko Bisulandu, B.-J.R.; Ilinca, A.; Rousse, D.R. Decarbonizing Arctic Mining Operations with Wind-Hydrogen Systems: Case Study of Raglan Mine. *Processes* **2025**, *13*, 3208. https://doi.org/10.3390/pr13103208

1. Introduction

As the world undergoes an ecological transition, countries that signed the Paris Agreement have committed to significantly reducing greenhouse gas (GHG) emissions by cutting the consumption of fossil fuels, which are known contributors to pollution. As a signatory, Canada accounted for 0.73 Gt CO_2 equivalent emissions in 2013, representing 1.95% of global GHG emissions [1]. The country has set ambitious targets to reduce national GHG emissions by 40–45% by 2030 and achieve net-zero emissions by 2050 [2–5]. This is how the Raglan Mine has set itself the goal to decarbonize its production system using renewable energy sources. This work evaluates the integration of a hybrid wind–hydrogen storage system as a pathway to progressively decarbonize the Raglan Mine's energy supply.

Renewable energy projects in autonomous northern Quebec face significant challenges related to climate, geography, technology, and storage. Extreme Arctic conditions, characterized by long, cold winters and short, cool summers, result in higher heating needs compared to other regions in Quebec. Technologies must also withstand freezing temperatures; for example, frost accumulation on wind turbine blades can severely reduce or even halt their operation [6].

Geographic factors also significantly impact the deployment of renewable energy in northern regions [7–10]. Communities and industries are small and sparsely distributed, making large-scale projects difficult without special measures. Many areas are isolated from the regional road network and rely on seasonal sea or air transport, which is limited in winter. This isolation increases the cost of imported goods, including diesel [11,12].

From a technical perspective, wind power is virtually the only renewable resource available in northern regions. Its integration is challenging, as technologies must withstand extremely low winter temperatures and occasional very strong winds. In northern Quebec, renewable penetration above 15–20% in microgrids already creates operational difficulties for network operators [13].

The fluctuating and intermittent nature of renewable energies challenges network stability and the balance between electricity supply and demand [14]. At high penetration levels, renewables can reduce short-circuit current and limit reactive power generation capacity, affecting grid reliability [15]. Additional concerns include power quality issues and resource variability, which may be further exacerbated by climate change.

Due to the intermittent nature of renewable energy sources, maintaining grid stability is one of the most critical technical challenges. Addressing this requires both regional cooperation and the deployment of energy storage systems. Storage enables the capture and release of surplus energy when production is insufficient, on hourly, daily, or seasonal scales [16]. This flexibility facilitates the integration of large-scale renewable energy sources, which explains the intense research interest in the field [17]. Energy storage is now widely recognized as a key enabler of the energy transition.

According to Multon et al. [18] and Li and Deusen [19], analyzing the fundamental characteristics of storage technologies is crucial. These include: (i) maximum charge and discharge power, often expressed as the ratio between useful and maximum power; (ii) energy capacity, typically in watt-hours, representing usable energy based on charge and discharge efficiency; (iii) overall efficiency, defined over one or more charge–discharge cycles; (iv) maximum number of cycles; and (v) the system's time constant.

Hydrogen storage is a promising solution for managing intermittency and surplus renewable electricity. The deployment of clean energy technologies increasingly depends on effective storage systems [20,21]. For example, Nagem et al. [22] analyzed a hybrid microgrid that combines solar PV, wind, and hydrogen storage to reduce costs and supply hydrogen for fuel cell vehicles

What makes Raglan Mine distinctive is that it is among the few Arctic mining operations to have already implemented a demonstration project combining wind turbines with hydrogen storage, providing unique operational insights (Figure 1).

Underground hydrogen storage is increasingly adopted in current energy systems [23–25]. Taiwo et al. [23] demonstrated that maintaining airtightness during storage, migration, and withdrawal is critical. Because hydrogen has a very low density at atmospheric conditions [26,27], storing it without compression would require extremely large volumes. For instance, 5 kg of hydrogen (equivalent in energy to 30 kg of gasoline) would occupy about 55 m^3, roughly the size of a private swimming pool.

To reduce storage volume, hydrogen density must be increased, yet storage remains challenging as it must be safe, sustainable, and efficient [28–31]. According to Mehrizi et al. [32], three critical criteria are affordability, moderate operating temperature, and adequate capacity. For Zhang et al. [33], Wang et al. [34], and Wallace et al. [35], the storage of hydrogen in compressed gas form is the most mature storage technique currently available. This approach involves compressing hydrogen to high pressures, up to 700 bar, and storing it in cylinders, bottles, or underground cavities.

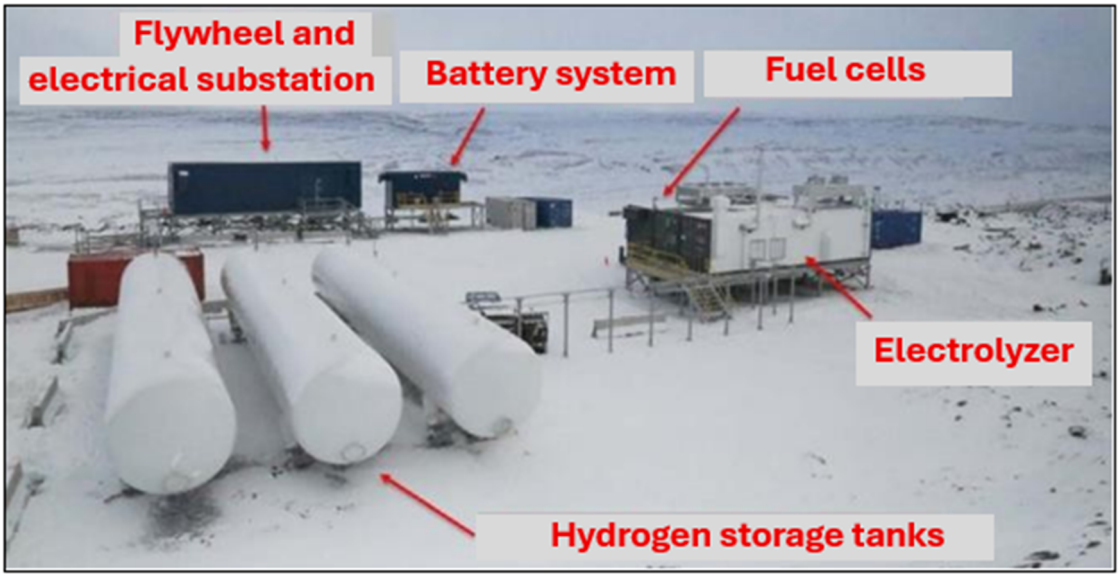

Figure 1. Storage facilities installed at Raglan Mine.

The storage system in the form of compressed gas has the advantage of being able to be implemented at ambient temperatures. For larger-scale storage, spherical tanks or underground pipeline installations are more suitable [36]. There are other techniques for storing hydrogen, including liquid storage [33,37,38] and solid hydrogen storage [39–42]. Figure 2 illustrates the various hydrogen production technologies and their applications in different sectors.

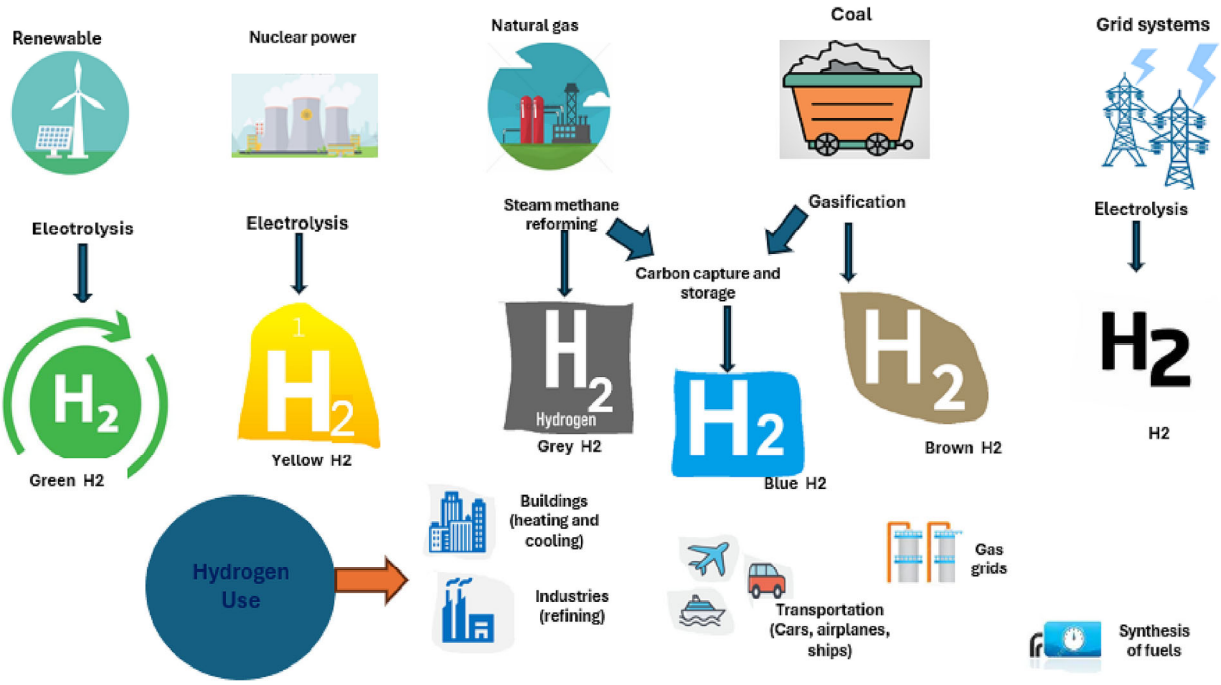

Figure 2. Hydrogen production and its industrial applications (Key performance indicators for each pathway are detailed in Table 1) [23]. (Reprinted from Journal of Energy Storage, with permission from Elsevier).

Table 1. Comparative indicators for main hydrogen production pathways, including emissions, efficiency, costs, production, and utilization [43–47].

Hydrogen Type/Pathway	GHG Footprint (kg CO_2-eq/kg H_2)	Energy Required & Efficiency (Typical)	LCOH—Indicative (Today → 2030+)	Production Today & 2030 Outlook	Utilisation by Sector (Today→2030)
Grey (natural gas, Steam Methane Reforming—SMR, unabated)	≈10–12 (NG SMR); coal-based ≈22–26	SMR uses ~44.5 kWh/kg (NG as process heat/feedstock); small electricity. Overall efficiency ~65–75% LHV (typical literature).	Highly gas-price dependent: ≈$0.6–1.0/kg at very low NG prices; ≈$2.9–4.2/kg at EU 2023 gas prices; +~$1/kg per $100/t$CO_2$eq carbon price (indicative).	Dominant: nearly two-thirds of 97 Mt (2023) from unabated NG; ~20% from coal. Low emissions <1%.	Mainly refining & chemicals today; new uses negligible (<1%). Shift to low emissions expected first in existing uses.
Blue (NG with Carbon Capture and Storage (CCS) SMR/ATR)	≈1.5–6.2 (capture rate & methane leakage dependent)	SMR + CCS: ~49 kWh/kg NG + ~0.8 kWh/kg el. at ~93% capture; ATR + CCS: ~47 kWh/kg NG + ~3.7 kWh/kg el. (93–94% capture).	Indicative: ≈$1.0–1.4/kg in low-gas regions; ≈$3.3–4.7/kg at high gas prices; less sensitive to carbon price at high capture rates.	Part of <1% low emissions today. Announced low-emissions H_2 could reach ~37–49 Mt/yr by 2030 (subject to FIDs/policy).	Expected to decarbonize current hydrogen uses first (refining, ammonia, methanol); potential growth in steel/DRI.
Green (electrolysis w/renewable sources)	≈0–0.8 from RE electricity manufacturing embedded emissions (up to ~2.7 incl. full embedded ranges)	Electrolysis ~50 kWh/kg (incl. compression to 30 bar); current Proton Exchange Membrane (PEM) systems ~55–58 kWh/kg. Efficiency ~60–70% (LHV).	Indicative today: often ~$3–8/kg (electricity-price driven). Targets: $1–2/kg by 2030s in favourable regimes (e.g., DOE "Hydrogen Shot" $1/kg by 2031).	<1% of supply today; rapid project pipeline, but many delays. Announced low-emissions H_2 (incl. green) ~37–49 Mt/yr by 2030 (uncertain realisation).	Today: minimal in final energy sectors; by 2030, growth expected in steel, heavy transport, shipping/aviation fuels where policy support exists.
Pink (electrolysis w/nuclear)	≈0.1–0.3 (depends on nuclear power lifecycle intensity)	Same electrolyzer needs as green (~50–55 kWh/kg). Potentially high utilisation if coupled to baseload nuclear.	Cost depends on nuclear power price & utilisation; ranges overlap green where low-cost nuclear is available.	Very small today; niche projects under discussion where stable nuclear baseload exists.	Potential in existing industrial hydrogen demand near nuclear plants; broader uptake depends on policy/regulation.
Turquoise (methane pyrolysis to H_2 + solid C)	≈2–16 (driven by NG upstream emissions & electricity for plasma/heating; no direct process CO_2)	Representative variant: ~62 kWh/kg NG + ~14 kWh/kg electricity (plasma).	Early-stage; costs uncertain and highly site/tech dependent; could compete with blue if low-emission power & cheap gas available.	Pilot/demonstration scale today.	Potential in chemicals and materials (solid carbon co-product markets); trajectory uncertain to 2030.

To complement Figure 2, Table 1 summarizes key quantitative indicators for each pathway, including typical carbon footprints, energy requirements and efficiencies, indicative levelized costs of hydrogen (LCOH), current and projected production capacities, and sectoral utilization shares. This additional information provides a broader context for comparing hydrogen options and situates the Raglan case study within global trends in hydrogen development [43–47].

As summarized in Table 1, hydrogen production pathways differ widely in emissions, energy requirements, costs, and sectoral applications, offering valuable benchmarks for evaluating their role in Arctic contexts. For Raglan Mine, these insights are directly tied to its overarching objective: the progressive decarbonization of operations through large-scale integration of renewable energy. Central to this strategy is the installation of a hydrogen storage system to manage the intermittency of wind power and reduce dependence on diesel. The mine's decarbonization efforts focus first on its electricity generation system, which is exceptional in both scale and remoteness. Located in Nunavik, northern Quebec, Raglan is one of the largest nickel producers in the Canadian Arctic, yet it is entirely off-grid and cannot access Quebec's predominantly hydroelectric network (97% hydro-based) [5]. Instead, it relies on an isolated system of diesel-fired power stations supplemented by two 3 MW wind turbines. This dependence on diesel not only drives high GHG emissions but also creates major logistical and financial challenges, as fuel must be shipped during limited seasonal windows at considerable cost. These unique conditions make Raglan Mine an ideal, though rare, case study for testing ambitious decarbonization strategies and for confronting the full range of technical, economic, and logistical barriers to renewable–hydrogen integration.

Raglan Mine has set ambitious decarbonization objectives, building on several years of practical experience with wind turbines and a pilot hydrogen storage system already in operation (Figure 1). This unique context provides not only real operational data but also valuable lessons learned under Arctic conditions, which form the foundation of the present study. Leveraging this rare combination of data and experience, the paper develops and compares six progressive decarbonization scenarios that extend beyond electricity generation to encompass heating, mining equipment, and transportation. By integrating hydrogen cost-reduction trajectories with site-specific operational realities, the study delivers new insights into the feasibility and scalability of hydrogen-based solutions in remote industrial microgrids. To our knowledge, this is one of the first applications of a staged, scenario-based techno-economic framework to a large industrial mining operation in the Canadian Arctic, thereby bridging the gap between conceptual models and the practical realities of implementing decarbonization strategies at scale. While this research focuses on hourly time steps and does not explicitly address short-term grid stability, it is worth noting that operational data and ongoing studies at Raglan include the use of battery energy storage systems (BESS) (Figure 1) for stabilization, which complements the hydrogen-based pathways analyzed here. More broadly, this work addresses the three challenges identified by Da Silva et al. [48]: (i) replacing fossil fuels with renewable sources, (ii) developing alternatives for hard-to-abate sectors, and (iii) eliminating CO_2 emissions through advanced mitigation strategies.

Du et al. [49] emphasize the need for a comprehensive transformation in the global electricity sector to achieve effective decarbonization. Similarly, Balaban et al. [50] argue that decarbonizing an energy system requires significant structural changes across the electricity production chain, including generation, transmission, and consumption, since this sector alone accounts for nearly two-thirds of total GHG emissions. Dongsheng et al. [51] further emphasize that ensuring a resilient and sustainable energy future by 2050 is only feasible if power generation integrates cost-effective and scalable renewable solutions. Meanwhile, Obiora et al. [52] and Roshan Kumar et al. [53] stress that a transition to low-carbon energy infrastructures must precede decarbonization efforts, as this remains the most effective approach to reducing the severe environmental impacts of climate change.

This article forms part of a broader research initiative assessing various energy storage technologies to support the decarbonization of remote mining operations in northern Quebec. In parallel with the present work on hydrogen storage, complementary studies have been conducted on redox flow batteries [54] and Pumped Hydro Storage System (PHSS) [55], with additional research underway on BESS. Each option is evaluated for its technical performance, economic viability, and environmental compatibility in off-grid Arctic contexts. Within this framework, the current paper focuses exclusively on the techno-economic feasibility of implementing hydrogen production and storage in Raglan Mine's hybrid electricity network.

In this study, a wind–hydrogen hybrid system is designed to progressively meet the mine's energy needs. Numerical simulations are used to explore six decarbonization pathways, ranging from partial decarbonization of the 25 kV network to full site-wide electrification, including heating, mining equipment, and transport. Declining hydrogen technology costs are also incorporated to capture anticipated technological progress and long-term deployment potential. The modeling adopts a macroscopic approach, centered on annual energy balances and investment requirements rather than short-term stability or power quality dynamics. All input data are drawn from Raglan Mine's 2021 energy report, ensuring that the analysis reflects real operational conditions.

While hybrid microgrids and hydrogen-based storage have been studied in remote and Arctic contexts, few works have addressed large-scale mining operations, where energy

demand extends beyond electricity to include transport, equipment, and heating. The originality of this work lies in (i) assessing hydrogen storage as a flexible enabler across successive decarbonization stages, (ii) explicitly considering cost-reduction trajectories for hydrogen technologies to evaluate long-term economic feasibility, and (iii) applying the framework to a real industrial case study in Northern Canada using recent operational data. This integrated approach provides new insights into the scalability and adaptability of hydrogen systems in Arctic microgrids, bridging the gap between conceptual analyses and practical decarbonization strategies for energy-intensive industries.

The remainder of this paper is organized as follows. Section 2 introduces the case study and details the methodological framework used for system modeling, including the definition of scenarios and cost assumptions. Section 3 presents the validation of the model against the baseline scenario derived from 2021 operational data. Section 4 presents the results of the decarbonization scenarios, focusing on system configuration, diesel displacement, and renewable energy penetration, while also evaluating the techno-economic viability. Section 5 synthesizes the key findings and identifies perspectives for future work, particularly regarding heating technologies, grid stability, and hydrogen storage innovations.

2. Methodology

This study focuses on the design of a hybrid energy system for Raglan Mine, integrating wind turbines with a hydrogen storage unit to progressively meet the site's energy needs. Numerical simulations are employed as the primary tool to size and assess the proposed system. To capture the range of possible configurations and optimize the role of hydrogen storage, several scenarios are evaluated. In recognition of the ongoing technological development of hydrogen solutions, additional scenarios incorporating projected cost reductions are also included. The analysis is conducted at a macroscopic level, emphasizing long-term energy balances rather than short-term constraints such as network stability, power quality, or frequency dynamics. Input data available from Raglan Mine covers operations for the year 2021. A brief overview of the Raglan site is provided in the following section.

2.1. Brief Description of the Raglan Mine Energy Network

Raglan Mine, located in the very north of Quebec, mines nickel and is part of the Glencore group. The Glencore group specializes in the mining industry and, although it participates in the global energy transition by making essential metals available, the group is a significant emitter of carbon dioxide (CO_2). The group has set itself the goal of reducing its carbon footprint by 15% by 2026, by 50% by 2035, and to achieve carbon neutrality by 2050. Raglan Mine is seeking solutions to decarbonize its production process. The mine is isolated from the electrical grid and faces extreme weather conditions, with temperatures reaching as low as $-60\ ^{\circ}C$ in winter. Each year, the Raglan Mine consumes more than 55 million liters (ML) of diesel. In 2021, for example, 59.8 ML were used. The energy produced by the diesel power plants is used to meet the needs of employees and the exploration, extraction, and primary processing of ore.

At present, diesel power plants supply approximately 98% of the mine's total energy demand, covering both electricity and heat requirements. The remaining 2% is provided by two on-site wind turbines (Enercon E82 E4, each with a capacity of 3 MW), which generated 8509 MWh each in 2021. The overall efficiency of the current energy system is estimated at 58.2%, with the remaining 41.8% dissipated as heat. However, this thermal energy is partially recovered and utilized to meet a share of the mine's heat needs.

Additional details of the electrical and heat grids configurations, load variation, and power sources production at Raglan Mine are available in recent publications [54,55].

2.2. Conditions and Limitations of the Scope of the Study

From a temporal perspective, the present decarbonization phase of the Raglan Mine extends over 15 years, from 2023 to 2037. This period coincides with the end of the mining site's operating contract, before a possible renewal, and aims to achieve a 50% reduction in its carbon footprint by 2035. It should be noted that the Raglan mine comprises a group of sites, some of which are connected to a 25 kV electrical network. Thus, during this phase (2023–2037), the decarbonization only concerns the 25 kV network. The 25 kV network is the electricity transmission network that connects all the mining sites around Katinniq (see Table 2). As such, this phase concerns all the generators and production stations at Kattiniq, Mine 2, Mine 3, and Qakimajurq that are connected to the network.

Table 2. Presentation of the sites and their connections to the network.

Site	Network Connection	Distribution of Production
Katinniq	Connected	68.9%
Mine 2	Connected	Wind turbines 9.5% Generators 3% Total 12.5%
Mine 3	Connected	2.8%
Qakimajurq	Connected	3.5%
Baie Déception (port)	Off-grid	3.3%
Kikialik	Off-grid	7.5%
Donaldson (airport)	Off-grid	0.5%

This 25 kV network alone accounts for 155,186,267 MWh, or 75% of diesel consumption, or 41.6 ML/year, for an emission of 113,000 tons of CO_2 equivalent (tCO_2eq). According to the 2021 energy data from the Raglan mine [55], the overall efficiency of electricity production by generators is 3.77 kWh/L, resulting in an electricity production efficiency of 35.4%, with the remainder of the energy being dissipated mainly in the form of heat. Only the heat from the EMD diesel generators is recovered. This is estimated at around 39% of the initial energy. Diesel heating, on the other hand, has an estimated efficiency of 75%. The average efficiency of vehicles and equipment is estimated at 35%.

Emissions from diesel use can be reduced by adopting several appropriate decarbonization techniques; this is the objective of Section 3, which details the decarbonization techniques used in this article, as well as the related economic aspects.

2.3. Different Technical and Economic Decarbonization Scenarios

To achieve optimal performance, it was decided to draw up several operating scenarios for the 25 kV network, including a wind farm and a hydrogen storage system. For each scenario, a technical and economic analysis was carried out to size the corresponding energy system, and thus determine: the number of wind turbines, the power of the electrolyzer, the total volume required to store energy in the form of hydrogen, the power of the fuel cell, and the economic viability of the project. Based on the Raglan Mine reference scenario, the different scenarios studied are as follows (Table 3):

1. Decarbonization of the 25 kV electrical network without decarbonizing the heat (heating and drying processes), which involves maintaining sufficient EMD diesel generators in operation to cogenerate all the heat required at the Raglan Mine.
2. Decarbonization of the 25 kV electrical network, including heating, without decarbonizing the drying process. This scenario involves decarbonizing the majority of the 25 kV electrical network, while ensuring sufficient EMD to continue providing heat for the ore drying process.
3. Decarbonization of the 25 kV electrical network, including heating and ore drying, involves decarbonizing the electricity and heat used by Mine Raglan.
4. Decarbonization of vehicles and equipment involves the reduction of carbon emissions from these sources.
5. Decarbonization of heavy transport focuses on the decarbonization of Raglan Mine's heavy transport, i.e., all its mining trucks.
6. Total decarbonization of Raglan Mine, which involves a comprehensive study of the entire Mine's decarbonization, regrouping scenarios 3, 4, and 5.

Table 3. Description of the different decarbonization scenarios.

Decarbonization Scenarios		Electricity	Heat		Vehicles and Equipment	Heavy Transport
			Heating	Drying		
1	25 kV electrical network without heat	Yes	No	No	No	No
2	25 kV electrical network without drying	Yes	Yes	No	No	No
3	25 kV electrical network with heat	Yes	Yes	Yes	No	No
4	Vehicles and equipment	No	No	No	Yes	No
5	Heavy transport	No	No	No	No	Yes
6	Total decarbonization	Yes	Yes	Yes	Yes	Yes

Separating this into several scenarios provides a better overview of the costs and dimensions of the systems based on the consumption items to be decarbonized.

The scenario dedicated to the decarbonization of mining vehicles and equipment, for example, considers all electrifiable consumption items, i.e., light vehicles (such as vans and surface vehicles) and all types of mining equipment. The energy consumption items identified include mining equipment (92.12%), surface vehicles (4.35%), and Toyota pickup trucks (3.53%). For this scenario, we created a virtual electrical load of 7.35 MW to model the consumption of vehicles and equipment at the Raglan mine. Since only aggregated energy data (not hourly data) is available for these charges, this 7.35 MW average considers their continuous operation, 24 h a day.

2.4. Choice of Computer Model

In this research, the HOMER Pro software (version 3.18) is used to model and simulate the hybrid network at the Raglan mine site. HOMER is a modeling software package developed by the U.S. National Renewable Energy Laboratory to assist in the design of microgrids. It facilitates various modeling processes for comparing technologies and their different applications. HOMER enables both system sizing for technical feasibility and economic optimization. To model easily in the HOMER software, it is essential to master the system under study, which is the objective of the following section.

2.5. Presentation of the System Studied

In this study, multiple scenarios are analyzed to identify a suitable pathway for decarbonizing the Raglan Mine. Scenario 1 is presented in detail, while results from the other scenarios are referenced for context. The proposed hybrid system integrates wind turbines with hydrogen technologies to partially replace diesel-based electricity. As shown in Figure 3, the system includes a hydrogen storage tank, a Proton Exchange Membrane Fuel Cell (PEMFC), Enercon E82 E4 wind turbines, a flywheel, a power converter, an electrolyzer, and a battery. The flywheel and battery, already installed at Raglan, are incorporated to ensure system stability and support dynamic operating phases. Their economic costs, however, are excluded from the present modeling.

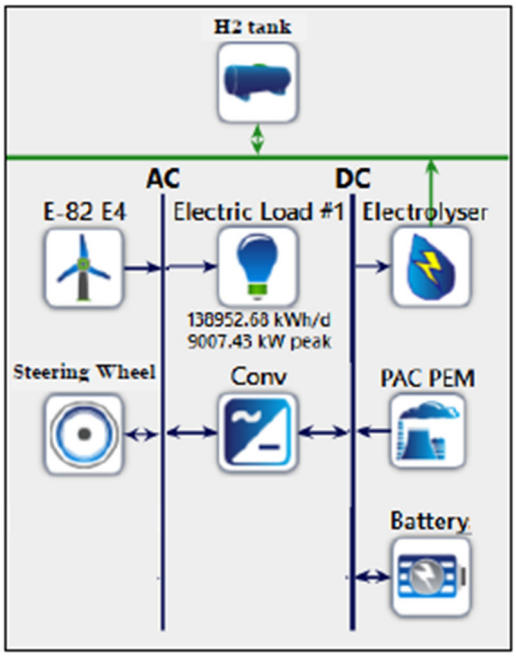

Figure 3. Modeling of the energy system components using HOMER software.

To improve clarity and readability, the primary technical and financial characteristics of the energy system components depicted in Figure 3 are summarized in a tabular format. These values are derived from operational data collected at Raglan Mine since 2021 and complemented with benchmark values from the literature on Arctic renewable energy and hydrogen systems. Short explanatory paragraphs highlight the role of each component in the overall decarbonization pathway. Financial data are presented in two currencies: CAD ($CAD), when derived directly from Raglan Mine's operational and financial records, and USD ($), when sourced from international datasets and literature sources, including the DOE, IEA, and IRENA. This distinction is maintained throughout the manuscript to preserve the integrity of the original data sources.

- Wind Turbine Technical and Financial Characteristics (based on real historical data at Raglan mine)

Wind power is central to the mine's decarbonization strategy. Enercon E82 E4 wind turbines, already operational on-site, were selected for their robustness under Arctic conditions. Their main technical and financial parameters are summarized in Table 4.

Table 4. Wind turbine technical and financial characteristics (Raglan Mine).

Parameter	Value	Notes
Rated power	3 MW per unit	Enercon E82 E4
Hub height	78 m	Cold-climate kit included
Rotor diameter	82 m	
Cut-in wind speed	2.5 m/s	
Rated wind speed	14 m/s	
Cut-out wind speed	28 m/s	
Annual production (2021)	8509 MWh/turbine	Measured on-site
Capacity factor	~32%	Based on 2021 data
Cold-climate adaptations	Anti-icing, reinforced materials, autonomous restart	
Capital Expenditure (CAPEX)	1700–1800 $/kW	Higher due to Arctic transport/foundations
Operating Expenditure (OPEX)	50–60 $/kW/year	Maintenance, spare parts
Lifetime	20–25 years	Reduced under Arctic conditions
Replacement/repowering	Blades, gearboxes mid-life	After 10–15 years

These turbines already contribute to reducing diesel dependence but face limitations from intermittency and icing, which motivates the complementary use of hydrogen storage.

- Diesel Generators Technical and Financial Characteristics

Diesel units currently form the backbone of Raglan's electricity and heat supply. While indispensable for continuous operations, they are also the largest source of costs and CO_2 emissions. Their key characteristics are summarized in Table 5.

Table 5. Diesel generator technical and financial characteristics (Raglan Mine).

Parameter	Value	Notes
Configuration	Multiple Caterpillar/EMD units	Total installed capacity 28 MW
Unit size	3.3 MW each	Average
Maximum demand covered	21 MW	Peak (2019–2021)
Efficiency	58.2%	~42% dissipated as heat (partly recovered)
Fuel	Diesel shipped & stored annually	
Operating profile	Baseload, frequent cycling	
Fuel cost (2021)	33 M$CAD	
Carbon tax (2021)	6.5 M$CAD	
O&M cost	2.5 M$CAD/year	~13% deviation vs. model
Total annual cost	42.5 M$CAD	Diesel + O&M + tax
Lifetime	20–25 years	Major overhauls 40–50k h
Fuel consumption	~12,000 L/day per unit	~4.4 ML/year/unit

These parameters highlight both the critical role and the limitations of diesel generation, underscoring the importance of progressive substitution with renewable–hydrogen systems.

- Battery Technical and Financial Characteristics

A lithium-ion battery system, combined with a flywheel (Figure 1), has already been deployed at Raglan. While not designed for long-term storage, it plays a crucial role in grid stabilization by smoothing fluctuations and providing rapid reserve capacity. Table 6 presents the main parameters.

Table 6. Technical and Financial Characteristics of the Battery System (Raglan Mine).

Parameter	Value	Notes
Technology	Lithium-ion (utility-scale)	With flywheel
Nominal capacity	200 kWh	
Power rating	200 kW	
Response time	ms to seconds	Grid support
Functions	Load balancing, spinning reserve, V/f stabilization	With flywheel
CAPEX	600–800 $/kWh	Higher in Arctic
OPEX	2% of CAPEX/year	
Lifetime	10–15 years	2% degradation/year
Replacement	After 8–10 years	Mid-life modules

The battery is not modeled as a primary long-term energy storage technology (this role being fulfilled by hydrogen), but rather as an auxiliary stabilizing component, ensuring reliable operation of the microgrid and complementing the flywheel system. Its economic cost was not included in the present modeling, since it is already operational at Raglan Mine.

- Electrolyzer Technical and Financial Characteristics

Hydrogen production is achieved with PEM electrolyzers, which are chosen for their modularity, responsiveness to variable wind inputs, and compatibility with Arctic deployment. Table 7 provides the adopted technical and financial parameters.

Table 7. PEM electrolyzer technical and financial characteristics [43–45].

Parameter	Value	Notes
Nominal capacity	1 MW	Modular
Production rate	20 kg H_2/h	At full load
Specific consumption	52–55 kWh/kg H_2	
Efficiency	60–65%	LHV
Operating pressure	30 bar	
Dynamic response	Sub-second	
CAPEX	1000–1200 $/kW	~30–40% reduction projected by 2030
OPEX	~3% of CAPEX/year	Maintenance, stack
Lifetime	60–80k h	10–15 years
Stack replacement	Every 7–10 years	30–40% CAPEX

These assumptions allow a realistic representation of hydrogen production costs and efficiency, which are key drivers of system economics.

- Hydrogen Tank Technical and Financial Characteristics

Produced hydrogen is stored in medium-pressure tanks, enabling seasonal and daily balancing as well as integration into electricity, heating, and transport uses. The main parameters are summarized in Table 8.

Table 8. Hydrogen storage tank technical and financial characteristics [43–45].

Parameter	Value	Notes
Storage type	Pressurized gas tanks	
Pressure	30 bar	Compatible with PEM
Storage capacity	Scenario-dependent	Hundreds of kg H_2
Role	Balances daily/seasonal fluctuations	
CAPEX	500–700 $/kg H_2 stored	Higher in Arctic
OPEX	2% of CAPEX/year	
Lifetime	20–30 years	Inspections 5–10 years
Scalability	Modular	

This storage system ensures flexibility across different decarbonization scenarios, though its cost remains a major sensitivity factor in the economic analysis.

- PEMFC Technical and Financial Characteristics

PEMFCs are used to reconvert stored hydrogen into electricity, thereby displacing diesel during periods of low renewable production. Their characteristics are shown in Table 9.

Table 9. PEMFC technical and financial characteristics [43–47].

Parameter	Value	Notes
Technology	LT-PEMFC	Modular
Nominal power	1 MW	
Efficiency	50–60%	Electrical
Start-up time	Seconds–minutes	Dynamic
Fuel	H_2 at 30 bar	
Integration	Backup power supply	
CAPEX	700–1400 $/kW	Higher Arctic costs
OPEX	~3% of CAPEX/year	Maintenance
Lifetime	20–30k h	~7–10 years
Stack replacement	Mid-life	
H_2 consumption	0.08–0.09 kg/kWh	

The modularity and fast response of PEMFCs make them particularly suitable for Arctic microgrids, although their high cost and limited lifetime remain significant challenges to their economic feasibility.

Together, these tables provide a comprehensive overview of the technical and financial assumptions underpinning the Raglan hybrid energy model. By combining operational

data with benchmark literature values, they ensure that the system simulations realistically capture the site's unique operating conditions. The following Section 2.6 describes how these parameters are integrated into the simulation model (Figure 3).

2.6. Mathematical Model

Several traditional equations were used to model the hybrid energy system, integrating hydrogen storage. Table A1 in the Appendix A provides a summary of the main equations used in this model.

2.7. Brief Analysis of Network Control and Stability

The extreme weather conditions at Raglan—such as turbine icing, intermittent production, and water freezing—create significant challenges for grid reliability and control. High renewable penetration reduces system inertia, affecting frequency and voltage stability. Although the current mine grid can limit deviations from nominal values, maintaining stability requires a close balance between electricity supply and demand at all times.

Large-scale renewable integration will therefore require detailed studies on grid stability, including the effects of intermittency and low inertia, as well as potential mitigation measures such as dynamic simulations, stochastic modeling, and the deployment of stabilization systems (e.g., Fault Ride Through and battery storage). While this paper provides an overview of these issues, detailed stability modeling is beyond its scope and will be addressed in future work.

3. Model Validation

The model is validated by comparing its results with operational data from Raglan Mine for the year 2021. Validation is carried out using four key indicators: (i) annual electricity production (MWh/year), (ii) diesel consumption (liters/year), (iii) CO_2 emissions (tons/year), and (iv) annual wind turbine output (MWh/year). Table 10 summarizes the reference data and validation criteria applied in this study.

Table 10. The 25 kV network, reference scenario (Raglan mine, 2021 data).

Raglan Mine 25 kV Network			
Parameters	**Model**	**Reality**	**Gap [%]**
Quantity of electrical energy produced in the year [MWh]	154.9	157	1.3
Number of liters of diesel consumed [ML]	37.2	37.3	0.4
Number of tCO_2eq [tons]	97,475	104,059	6.4
Wind power production [MWh]	17,042	17,017	0.01

The simulation results show good agreement with the actual operational data from Raglan Mine, confirming the validity of both the modeling approach and the use of HOMER software. The modeled outputs closely match the reference values for energy production, diesel consumption, and wind generation, with only a slight underestimation observed in the reported CO_2 emissions.

Table 11 compares the modeled results with the financial data reported by Raglan Mine for 2021. A 13% difference is observed in OPEX, which can be attributed to the way HOMER software optimizes the use of diesel engines while supplementing heat production with auxiliary diesel heaters not accounted for in this study. This discrepancy is not considered critical, as the modeled diesel fuel costs are in very close agreement with the

mine's reported data, with a difference of less than 1%. Overall, the total cost comparison confirms the robustness of the model, and the validated results are presented in detail in Section 4.

Table 11. Reference model cost study (Raglan mine).

Year 2021			
Costs	**Model**	**Mine Data**	**Gap [%]**
OPEX	2,162,000 $	2,494,000 $	13%
Cost of diesel	32,896,000 $	33,010,000 $	0.3%
Carbon tax	6,500,000 $	N/A	N/A
Total	42,507,800 $	N/A	N/A

N/A, not applicable.

4. Results and Discussion

4.1. Data and Assumptions of the Model

This section presents the data and assumptions used in the study. Table 12 summarizes Raglan Mine's energy consumption requirements, which serve as the basis for appropriately sizing the renewable energy integration and the hydrogen storage system.

Table 12. Assessment of the mine's energy needs (Raglan mine).

Section	Energy Consumed	Data	Average Power in MW	Percentage
Electricity	Electricity	Hourly schedules	17.8	41.2%
Drying the ore	Heat	Averages	6.75	15.6%
Glycol heating	Heat	Hourly schedules	6.59	15.2%
Auxiliary heating	Heat	Averages	2.08	4.8%
Mining equipment	Electricity	Averages	6.77	15.7%
Surface vehicles	Electricity	Averages	0.32	0.7%
Toyota pickup trucks	Electricity	Averages	0.26	0.6%
Mining trucks	Fuel	Averages	2.63	6.2%
Total	N/A	N/A	43.2	100%

N/A, not applicable.

Table 13 summarizes Raglan Mine's electricity consumption over the period 2019–2021, showing a maximum power demand of 21 MW. For this study, the 2021 dataset is used as the reference for modeling and simulation.

The glycol heating system supplies thermal energy to all areas where personnel live and work, including offices, accommodation facilities, and mining operation sites. Currently, this heating demand is primarily met by diesel generator units (DGUs), supplemented by two dedicated diesel-fired boilers. Unlike the drying process and auxiliary heating, the glycol heating load cannot be represented as a constant value, as it varies considerably throughout the year, with peak demand occurring during the winter months. According to data provided by Raglan Mine, the glycol heating system requires a maximum power of 14.1 MW and consumed 55.3 GWh in 2021, which enabled the reconstruction

of the hourly heating demand profile. The techno-economic parameters for hydrogen equipment (PEMFC and PEM-based electrolyzer) used in this study are based on published projections and market analyses. Given the early commercial stage of large-scale PEM deployment, current costs remain relatively high (see Section 2.5), but significant reductions are anticipated due to mass production, supply chain maturation, and efficiency improvements. Therefore, the study uses the following assumptions on the financial evolution of PEM technology.

Table 13. Mine electricity consumption in 2019, 2020, and 2021 (Raglan mine).

	Power Consumption		
	Year 2019	**Year 2020**	**Year 2021**
Maximum power [kW]	20,390.85	20,886.96	21,007.42
Electricity consumed [kWh]	146,370,985	144,836,291	154,959,758

PEMFC [43–47]:

- System CAPEX (2020): 700–1400 $/kW, reflecting costs of small- to medium-scale demonstration projects and the immaturity of supply chains.
- System CAPEX (2050): projected to fall below 200 $/kW, according to international roadmaps (IEA, Hydrogen Council, DOE targets), driven by scale effects, standardization, and improved stack durability.
- OPEX: expected to decrease proportionally with CAPEX, although maintenance of membranes and balance-of-plant will remain significant.
- Lifetime: expected to increase from ~20,000–30,000 h today to >60,000 h in the long term, reducing replacement frequency and lifecycle costs.

Electrolyzers (PEM-based)

- System CAPEX (2020): 1000–1200 $/kW, depending on scale and region.
- System CAPEX (2050): projected to decrease to 200–500 $/kW, following learning curves similar to those of renewable technologies (solar PV, wind).
- Efficiency: expected to rise from 60 to 65% today to >75% by 2050, further improving hydrogen production costs.

The combined CAPEX reduction and efficiency gains are expected to bring green hydrogen production costs below 2 $/kg by 2050 in favorable wind conditions. The underlying assumptions are (i) a learning rate of 12–18% is assumed for both PEMFC and PEM electrolyzers, meaning that costs decrease by this percentage with each doubling of installed cumulative capacity; (ii) projections also assume progressive industrial scaling, international policy support for hydrogen, and reductions in material costs (e.g., reduced platinum loading in PEMFC stacks); (iii) remote site deployment (e.g., Raglan Mine) is expected to add a cost premium (transport, installation, maintenance), but the general downward global trend remains valid.

4.2. Model Results for Scenario 1, the Decarbonization of the 25 kV Electric Grid Without Heat

This scenario assesses the partial decarbonization of the mine by focusing exclusively on the 25 kV electrical network, while maintaining a minimum number of diesel generators (EMDs) in operation to ensure the heat supply for the glycol heating and ore drying. Two sub-cases are considered:

4.2.1. Case 1—Constant Operation of Four EMDs

In this configuration, four 3 MW EMD units operate continuously throughout the year, resulting in a nominal installed capacity of 12 MW. The hybrid system, designed to cover

the residual load, comprises 14 wind turbines (42 MW), a 14 MW electrolyzer, a 67,000 kg hydrogen tank, and a 9.2 MW PEMFC, all complemented by converters (Table 14).

Table 14. System configuration for Scenario 1 (Case 1 and Case 2).

Component	Case 1	Case 2
Number of Wind Turbines	14	22
Wind Turbine Power [MW]	42	66
PEM electrolyzer [MW]	14	20
Storage tank [kg]	67,000	147,000
PEMFC [MW]	9.2	13.8
Converter [MW]	14.4	20.2

Simulation results indicate that EMDs provide 43.9% of annual electricity (104.2 GWh), while wind turbines supply 50.3% (119.2 GWh), and the PEMFC contributes 5.8% (13.8 GWh). This configuration achieves a renewable penetration of 56.1%, but also generates 31% excess electricity that is not valorized in this case (Table 15). Diesel consumption remains significant (approximately 27 ML annually), though it represents a reduction of about 10.3 ML compared to the reference system.

Table 15. Energy results for Scenario 1 (Case 1 and Case 2).

Electricity Production on the 25 Kv Network	Case 1		Case 2	
	[GWh]	[%]	[GWh]	[%]
By the EMD	104.2	43.9	57.8	18.2
By the wind turbines	119.2	50.3	238.6	75.1
By PEMFC	13.8	5.8	29.5	9.3
Total	237.4	100	317.8	100
Penetration of renewable electricity into the network	133.1	56.1	268.1	84.4
Excess electricity	41.5	31 *	75.4 **	+23.7
Diesel consumption reduction [ML]	10.3		22	
CO_2 reduction estimation [tCO_2eq]	26,989		57,646	

* % more than the total renewable production consumed by the network. ** % of the total production of renewable electricity produced on the network.

Economically, the total investment cost is estimated at 141.3 M$, with wind turbines and the hydrogen tank representing the most significant shares (Table 16).

Table 16. Economic results for Scenario 1 (Case 1 and Case 2).

Components	Total CAPEX				OPEX Per Year			
	In M$		In %		In M$		In %	
	Case 1	Case 2	Case 1	Case 2	Case 1	Case 2	Case 1	Case 2
E-82 E4 wind turbine	73.5	147.0	52.0	47.0	2.4	4.8	74.8	73.9
Electrolyzer	9.8	17.4	6.9	5.6	0.4	0.7	12.3	10.8

Table 16. *Cont.*

Components	Total CAPEX				OPEX Per Year			
	In M$		In %		In M$		In %	
	Case 1	Case 2	Case 1	Case 2	Case 1	Case 2	Case 1	Case 2
H_2 tank	40.2	115.2	28.5	36.8	0.2	0.6	6.3	8.9
Fuel cell	9.2	16.7	6.5	5.3	0.1	0.3	4.3	4.2
Converter	8.6	16.5	6.1	5.3	0.1	0.1	2.3	2.1
Total system	141.3	312.7	100	100	3.2	6.4	100	100

The payback period is 12.8 years, and although the Net Present Value (NPV) becomes positive after 20 years, discounted values remain negative in the shorter term (Table 17).

Table 17. NPV study for Scenario 1 (Case 1 and Case 2).

Index	Over 15 Years		Over 20 Years	
	Case 1	Case 2	Case 1	Case 2
NPV	15.4	27.83	82.7	173.8
Discounted NPV	−43.5	−104.9	−19.9	−54.0
Payback period [years]	12.8		12.8	

4.2.2. Case 2—Optimized Operation of EMDs

In this configuration, the output of the four EMDs is adjusted according to the seasonal heat demand. During periods of lower thermal demand, fewer EMDs are used, allowing for the integration of more renewable electricity. The optimized system requires 22 wind turbines (66 MW), a 20 MW electrolyzer, a 147,000 kg hydrogen tank, and a 13.8 MW PEMFC (Table 14).

This setup increases renewable penetration to 84.4%, with wind turbines producing 238.6 GWh (75.1%), EMDs 57.8 GWh (18.2%), and PEMFC 29.5 GWh (9.3%). Excess renewable production reaches 23.7% of total generation (Table 15). Diesel use drops substantially, resulting in a savings of nearly 22 ML per year compared to the baseline.

The economic assessment indicates higher costs, with a total investment of 312.7 M$, primarily driven by wind turbines (47%) and the hydrogen tank (37%) (Table 16).

The payback period is similar (12.8 years), but the NPV remains negative under standard discounting assumptions, turning positive only when subsidies or favorable financing conditions are considered (Table 17).

In Case 1, wind turbines account for the largest share of costs, representing over 50% of the total CAPEX and more than 70% of annual OPEX. The hydrogen tank is the second-largest investment, contributing nearly 30% of CAPEX. In Case 2, the cost distribution remains similar, although the share of wind turbines decreases slightly to 47% of CAPEX. As in the first case, the hydrogen tank remains the second-largest capital item, representing about 36% of total investment costs.

For both cases, the estimated return on investment (ROI) is 12.8 years. A more detailed viability analysis based on the NPV (Table 17) shows that when the discount rate (here 8%) and inflation (2%) are included, the NPV remains negative after 15 years. It is essential to note that this indicator serves as a forecasting tool, subject to significant uncertainty. Without discounting and inflation, the NPV results are much more favorable.

Overall, the ROI remains attractive since the mine's operations are expected to continue for at least 15 years. Moreover, with the addition of potential Canadian government subsidies to support decarbonization, both Case 1 and Case 2 would likely become profitable.

Scenario 1 demonstrates that significant reductions in diesel consumption and CO_2 emissions can be achieved by integrating wind power and hydrogen storage while maintaining a minimum number of EMDs to supply heat. The optimized case achieves a renewable penetration of over 80% and substantial fuel savings but requires more than double the CAPEX of the constant-operation case. In both cases, economic viability is sensitive to discount rates and financial assumptions, but payback times are within the mine's expected lifetime. The analysis highlights that valorization of excess electricity (e.g., through heating or hydrogen export) and potential government support could play a decisive role in improving the economic outlook.

4.3. Model Results for Scenario 2, the Decarbonization of the 25 kV Electric Grid with Glycol Heating and Without Ore Drying

This scenario examines the decarbonization of the entire 25 kV electrical network and the glycol heating system, while maintaining two EMD generators to supply the high-temperature heat (350 °C) necessary for the drying process. The retained EMDs provide 6 MW of carbon-based electricity and heat. Two cases are studied:

- Case 1: Use of PEMFC, with thermal demand aggregated into the electrical load under the assumption that 1 kWh of electricity can substitute 1 kWh of heat.
- Case 2: Use of Solid Oxide Fuel Cell (SOFC) fuel cells with cogeneration, separating electricity and heat production, and supplemented by diesel boilers where necessary.

4.3.1. Case 1: Use of PEMFCs

The optimized system includes 47 wind turbines (141 MW), a 30 MW electrolyzer, a 295,000 kg hydrogen tank, and a 29 MW PEMFC.

Energy results: Annual production is 493 GWh, of which 81% is supplied by wind turbines, 8% by PEMFCs, and only 10.6% by EMDs. Renewable penetration reaches 89%, but excess electricity represents more than 33% of renewable generation. Diesel consumption remains at 12.9 ML annually, corresponding to savings of 24.4 ML compared to the baseline.

Economic results: The total investment is estimated at 484.5 M$, dominated by wind turbines (51% of CAPEX, 80% of OPEX) and hydrogen tanks (37% of CAPEX). The ROI is 16.6 years. The NPV, even without discounting, remains weak, and the discounted NPV is negative over 15–20 years, indicating limited economic viability for this configuration.

4.3.2. Case 2: SOFC with Cogeneration

In this case, the system configuration presented in Figure 3 is slightly modified, as shown in Figure 4. The optimized configuration comprises 28 wind turbines (84 MW), a 25 MW electrolyzer, a 120,000 kg hydrogen tank, and a 16 MW SOFC, along with additional diesel boilers.

Energy results: The system generates 460 GWh annually, with 79.6% from wind turbines, 9% from SOFCs, and 11.4% from EMDs, yielding a renewable penetration of 88.6%. Diesel savings are approximately 24.3 ML per year. For heat production, SOFCs contribute 17%, while EMDs provide 52.5%, and boilers account for 30%. With current configurations, renewable heat penetration is modest (17.4%); however, replacing diesel boilers with electric boilers supplied by surplus electricity could increase this to nearly 60%.

Economic results: The total CAPEX is 268.9 M$, with wind turbines (55%) and hydrogen tanks (27%) as the main cost drivers. The ROI is 11.6 years. Incorporating a Thermal Charge Controller (TCC, 36 MW) significantly improves results by converting excess elec-

tricity into heat, reducing boiler diesel use by over 40% (saving ~1.9 ML annually). With this addition, the ROI decreases to 10.7 years, and the non-discounted NPV becomes strongly positive.

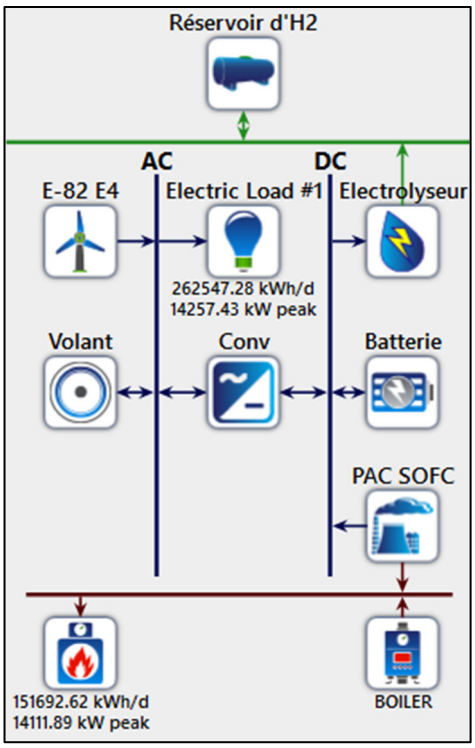

Figure 4. Modeling of energy system components for Scenario 2, Case 2.

Scenario 2, with summary results presented in Table 18, demonstrates the potential for deeper decarbonization of the Raglan mine's electrical and glycol heating systems while excluding the most technically challenging process (drying). Case 1 achieves high renewable penetration but at very high costs and poor economic viability. Case 2, based on SOFC cogeneration, offers a more balanced solution, particularly when complemented by a TCC that valorizes surplus renewable electricity as heat. When a TCC is introduced, a significant portion of surplus electricity is redirected to the glycol heating network. This reduces boiler diesel consumption by approximately 40% and improves the ROI (from 11.6 to 10.7 years). This demonstrates that the valorization of excess electricity can substantially improve both energy and economic performance.

Table 18. System configurations and primary energy and economic results for Scenario 2 (Case 1 and Case 2).

Case	System Configuration	Renewable Penetration	Diesel Savings	CAPEX (M$)	ROI (Years)
Case 1 (PEMFC)	47 WT (141 MW), 30 MW electrolyzer, 295,000 kg H_2 tank, 29 MW PEMFC	89%	24.4 ML	484.5	16.6
Case 2 (SOFC)	28 WT (84 MW), 25 MW electrolyzer, 120,000 kg H_2 tank, 16 MW SOFC, diesel boilers	88.6%	24.3 ML (+1.9 ML with TCC)	268.9	11.6 (10.7 with TCC)

4.4. Model Results for Scenario 3, Full Decarbonization of the 25 kV Electricity and Heat Networks

Scenario 3 explores the complete decarbonization of the 25 kV electricity and heat network at Raglan Mine by potentially removing all diesel generators. Both the 25 kV electricity grid and the thermal (glycol heating and ore drying) network must therefore be supplied exclusively from renewable sources and hydrogen-based technologies. Two cases are examined:

- Case 1: PEMFC (no cogeneration): Since PEMFCs only produce electricity, the electrical and thermal loads are combined into a single demand profile. The assumption is made that 1 kWh of electricity can offset 1 kWh of heat demand.
- Case 2: SOFC (with cogeneration): SOFCs can produce both electricity and heat simultaneously. In this case, the electrical and thermal demands are modeled separately, with diesel boilers supplementing heat production when renewable generation is insufficient.

4.4.1. Case 1: Use of PEMFCs

System sizing: The optimal configuration requires 67 wind turbines, coupled with a hydrogen storage system of 400 t, a 69 MW electrolyzer, and 42 MW of PEMFCs.

Energy results: The system provides 644 GWh annually, entirely from renewable sources. Wind generation dominates (88.6%), while PEMFCs supply 11.4%. Excess electricity reaches 160 GWh (≈25% of annual production). All diesel consumption (37.3 ML) is eliminated.

Economic results: The total CAPEX is estimated at 705 M$, with wind turbines representing approximately 50% of investment and 76% of OPEX. Hydrogen storage accounts for 34% of CAPEX. The ROI is 15.5 years. NPV remains negative over 15 years but becomes positive beyond 20 years, suggesting long-term viability if subsidies or cost reductions materialize.

4.4.2. Case 2: SOFCs with Cogeneration

System sizing: The optimized system requires 35 wind turbines, a 245 t hydrogen tank, a 49 MW electrolyzer, and 22 MW of SOFCs (configuration illustrated in Figure 4).

Energy results: Annual electricity production reaches 343 GWh, fully renewable, with wind turbines contributing 86.8% and SOFCs 13.2%. Excess electricity is lower than in Case 1 (16.4%). In terms of heat, SOFC cogeneration covers 27.2% of the mine's heating demand, while diesel boilers provide 72.8%, consuming approximately 8.7 million liters of diesel annually. Introducing a TCC to convert excess electricity into heat reduces diesel boiler use by 26% (≈2.3 ML saved).

Economic results: The total CAPEX is 411 M$, significantly lower than in Case 1 due to fewer wind turbines. Wind turbines remain the dominant cost (45% of CAPEX, 64% of OPEX), followed by hydrogen storage (36%). The ROI is 12 years without a TCC, improving to 11 years with a TCC. The NPV remains negative after 15 years but trends toward viability in the long run.

Scenario 3, as synthesized in Table 19, demonstrates that the complete decarbonization of Raglan Mine's electricity and heat networks is technically feasible. Case 1 (PEMFC) ensures complete decarbonization but requires substantial investments and faces lengthy payback times. Case 2 (SOFC cogeneration) appears more balanced, with significantly reduced CAPEX and OPEX, shorter ROI, and the additional benefit of producing renewable heat, especially when complemented by a TCC. However, both cases highlight that without subsidies or significant cost declines in hydrogen technologies, achieving complete decarbonization remains economically challenging.

Table 19. System configurations and primary energy and economic results for Scenario 3 (Case 1 and Case 2).

Element	Case 1 (PEMFC, No Cogeneration)	Case 2 (SOFC, Cogeneration)
Wind turbines	67 (201 MW)	35 (105 MW)
Electrolyzer capacity	69 MW	49 MW
Hydrogen storage	400 t	245 t
Fuel cell capacity	42 MW (PEMFC)	22 MW (SOFC)
Electricity production	644 GWh (100% renewable)	343 GWh (100% renewable)
Heat production	Electricity is assumed equivalent to heat demand	113 GWh (27% renewable from SOFC cogeneration, 73% diesel boilers)
Excess electricity	160 GWh (24.8%)	56 GWh (16.4%)
Diesel consumption avoided	37.3 ML (100%)	37.3 ML (100%) + 2.3 ML with TCC
Total CAPEX	705 M$	411 M$
Main CAPEX contributor	Wind turbines (50%)	Wind turbines (45%)
ROI/NPV (15 years)	15.5 years/NPV negative	12 years (11 with TCC)/NPV negative

4.5. Model Results for Scenario 4, Decarbonization of Mining Vehicles and Equipment

This scenario evaluates the feasibility of fully decarbonizing mining vehicles and equipment at Raglan Mine by electrifying their operations. The total additional electrical load is estimated at 7.35 MW, of which mining equipment accounts for over 92%, while surface vehicles and light trucks contribute the remaining 8%. Given their continuous operation, these loads were modeled as a constant demand throughout the year.

A virtual electrical load of 7.35 MW was added to represent the combined consumption of vehicles and mining equipment. As detailed operational profiles were unavailable, the demand was averaged over 24 h, reflecting the 24/7 utilization typical of Raglan Mine's fleet. This modeled load was then integrated into the hybrid renewable-hydrogen system for optimization.

The main results of this scenario are presented in Table 20 (system configuration, energy performance, economic performance, ROI, and NPV).

Table 20. System configuration, energy, and economic performance for Scenario 4.

Element	Case (PEMFC System)
Wind turbines	19 (54 MW)
Electrolyzer capacity	11 MW
Hydrogen storage	100 t
Fuel cell capacity	8.5 MW (PEMFC)
Electricity production	179 GWh (100% renewable) 90.6% wind turbines and 9.4% PEMFC
Heat production	Not applicable
Excess electricity	72 GWh (40%)
Diesel consumption avoided	8.5 ML (100%)
Total CAPEX	182.4 M$ (55% wind turbines, 33% H_2 tank)
Total OPEX	3.2 M$ (79% wind turbines, 7.3% H_2 tank, 7.6% electrolyzer)
ROI/NPV	years/NPV negative (15 years)

4.6. Model Results for Scenario 5, Decarbonization of Heavy Transport

This scenario provides an order-of-magnitude estimation for sizing a system capable of producing sufficient hydrogen to supply the mine's heavy trucks throughout the year. While not a detailed replacement study of the truck fleet, it offers a global perspective on the energy production infrastructure required for future decarbonization of heavy transport. Beyond GHG reduction, switching to hydrogen trucks would also reduce particle emissions and the need for mine ventilation, which currently accounts for nearly 20% of the mine's electricity demand. It is worth mentioning that the system is fully powered by wind turbines, enabling 100% renewable hydrogen production.

The main results of this scenario are presented in Table 21 (system configuration, energy performance, economic performance, ROI, and NPV).

Table 21. System configuration, energy, and economic performance for Scenario 5.

Element	Case (Hydrogen Trucks)
Wind turbines	8 (24 MW)
Electrolyzer capacity	15 MW
Hydrogen storage	75 t
Converter	15 MW
Fuel cell capacity	(H_2 only for trucks)
Electricity/H_2 production	68 GWh H_2 (100% renewable)
Heat production	Not applicable
Excess electricity	Not applicable
Diesel consumption avoided	5.5 ML (100%)
Total CAPEX	114 M$ (35.7% wind turbines, 39.3% H_2 tank)
Total OPEX	2.1 M$
ROI/NPV	17.7 years/NPV negative (for 15 and 20 years)

4.7. Model Results for Scenario 6, Total Decarbonization of Raglan Mine

This scenario assesses the complete decarbonization of the Raglan Mine, encompassing the 25 kV electrical and thermal network, mining trucks, equipment, light vehicles, Toyota pickups, and underground heating systems. Two cases are considered: the use of PEMFCs (Case 1) and the use of SOFCs with cogeneration (Case 2).

The main results of this scenario are presented in Table 22 (system configuration, energy performance, economic performance, ROI, and NPV). For Case 2, with the integration of a TCC, diesel savings are enhanced, but the discounted NPV remains negative over 20 years.

Table 22. System configuration, energy, and economic performance for Scenario 6 (Case 1: PEMFCs; Case 2: SOFCs).

Element	Case 1 (PEMFC, No Cogeneration)	Case 2 (SOFC, Cogeneration)
Wind turbines	102 (306 MW)	66 (198 MW)
Electrolyzer capacity	90 MW	59 MW
Hydrogen storage	500 t	345 t
Fuel cell capacity	54 MW (PEMFC)	33 MW (SOFC)
Electricity production	966 GWh (100% renewable) (89.7% wind turbines; 10.3% PEMFC)	628 GWh (100% renewable) (89.6% wind turbines, 10.4% SOFC)
Heat production	Electric heating assumed	134 GWh (29% renewable, 71% diesel; +43% with TCC)
Excess electricity	281 GWh (21%)	183 GWh (29%)
Diesel consumption avoided	53.3 ML (100%)	42.8 ML (80%); 48.4 ML with TCC

Table 22. *Cont.*

Element	Case 1 (PEMFC, No Cogeneration)	Case 2 (SOFC, Cogeneration)
Total CAPEX	975 M$	655 M$
Main CAPEX contributors	Wind turbines (55%) Hydrogen tank (31%)	Wind turbines (53%)
Total OPEX	22 M$	14.5 M$
Main OPEX contributors	Wind turbines (80%), Electrolyzer (8%), Hydrogen tank (7%)	Wind turbines (77%), Electrolyzer (9%), Hydrogen tank (7%)
ROI	21.1 years	19.2 years (14.8 with TCC)
NPV (15 years)	Negative	Negative

5. Discussion

The purpose of this section is to synthesize the results from the six scenarios presented earlier, highlighting their energy and economic implications, and identifying pathways for improving the realism and feasibility of decarbonization strategies at Raglan Mine.

5.1. Energy Comparison of Different Scenarios

The six scenarios assessed in this work do not all share the same scope. Scenarios 1 to 3 focus on the decarbonization of the 25 kV network (electricity and heat), Scenarios 4 and 5 address transport and mining equipment, while Scenario 6 considers full decarbonization of the mine, combining all previous loads. The results (Table 23) demonstrate that it is technically possible to size a renewable-based system capable of meeting all of Raglan Mine's energy needs. Several conclusions emerge:

- The mine can theoretically be supplied entirely by renewable energy, provided that heating processes are electrified.
- The integration of SOFCs in cogeneration partially addresses thermal needs but still requires complementary heating.
- The addition of a TCC significantly improves the integration of renewable heat, in some cases, almost doubling the share of renewable heat.
- Excess electricity, ranging from 20% to 30% in several scenarios, should not be considered wasted. As demonstrated in Scenario 2 with TCC integration, redirecting this surplus into thermal loads can increase renewable heat penetration by nearly 40%. Other potential pathways for valorization include charging of electric auxiliary vehicles and future hydrogen-based exports (e.g., ammonia), although these remain at a conceptual stage in the Arctic context.

Table 23. Decarbonization levels across the different scenarios.

The Scenarios	Number of ML of Diesel Saved	Decarbonization of the Electricity Production of the 25 kV Network	Integration of Renewable Heat into the 25 kV Network	Decarbonization of Total Energy Consumption in Raglan Mine
S1 C1	10.3	27.6%	0.0%	19.3%
S1 C2	22	59.0%	0.0%	41.3%
S2 C1	24.4	65.4%	55.3%	45.8%
S2 C2	20.9	56.0%	17.4%	39.2%
S2 C2 TCC	22.8	61.1%	57.0%	42.8%

Table 23. *Cont.*

The Scenarios	Number of ML of Diesel Saved	Decarbonization of the Electricity Production of the 25 kV Network	Integration of Renewable Heat into the 25 kV Network	Decarbonization of Total Energy Consumption in Raglan Mine
S3 C1	37.3	100.0%	100.0%	70.0%
S3 C2	28.7	76.9%	27.2%	53.8%
S3 C2 TCC	31	83.1%	47.5%	58.2%
S4	5.5	N/A	N/A	10.3%
S5	8.5	N/A	N/A	15.9%
S6 C1	53.3	100%	100%	100.0%
S6 C2	42.8	100%	29.2%	80.3%
S6 C2 TCC	48.4	100%	59.4%	90.8%

Where Si = Scenario i (i = 1 to 6); Cj = Case j (j = 1 to 2); N/A = not applicable.

5.2. Environmental and Economic Comparisons

From an environmental and economic standpoint, the results highlight strong contrasts between scenarios. Key indicators such as diesel savings and CAPEX are summarized in Table 24. Some observations:

- Scenarios utilizing PEM technologies generally enable higher decarbonization levels, albeit at higher costs.
- Scenarios with SOFC technologies offer better efficiency in terms of CAPEX, but renewable heat penetration remains more limited.
- Ambitious projects such as Scenario 6, Case 1 (total decarbonization with PEM), achieve the complete replacement of diesel but require nearly $1 billion in investment.
- The valorization of surplus electricity has a decisive influence on project viability. While unutilized energy reduces system efficiency and increases LCOE, strategies such as TCC integration improve economic outcomes by lowering diesel consumption. Although hydrogen export and ammonia production are not modeled in detail here, they represent longer-term opportunities to monetize excess electricity in Arctic mining operations.

Table 25 presents ROI alongside both discounted (considering the discount and inflation) and undiscounted NPVs. Results show that the more ambitious the scenario, the less economically attractive it becomes. Longer ROI and highly negative discounted NPVs characterize the full decarbonization cases. None of the discounted NPVs are positive over 15–20 years. However, this outcome must be interpreted with caution:

- Discount and inflation rates are uncertain. In the simulations, the discount rate was set at 8% and inflation at 2%.
- Diesel price volatility plays a significant role. While current market conditions do not suggest significant long-term price decreases, the assumed values have a strong impact on NPVs.

Notably, the analysis does not include governmental subsidies or carbon pricing policies, which could significantly improve project viability. Although the Canadian carbon tax was initially projected to rise from $CAD 65/t$CO_2$eq in 2023 to $CAD 170/t$CO_2$eq by 2030, recent political changes and the uncertain international context make it challenging to adopt reliable assumptions at this stage.

Table 24. Comparisons of environmental effects and investment level across the different scenarios.

The Scenarios	ML of Diesel Saved	CAPEX
S1 C1	10.3	141.3
S1 C2	22	312.1
S2 C1	24.4	484
S2 C2	20.9	269
S2 C2 TCC	22.8	269
S3 C1	37.3	705
S3 C2	28.7	410
S3 C2 TCC	31	410
S4	5.5	114.3
S5	8.5	182.4
S6 C1	53.3	974
S6 C2	42.8	655
S6 C2 TCC	48.4	655

Where Si = Scenario i (i = 1 to 6); Cj = Case j (j = 1 to 2).

Table 25. NPV across scenarios.

The Scenarios	ROI (Years)	Discounted NPV Over 15 Years (M$)	NPV (M$)
S1 C1	9.5	−43.5	15.4
S1 C2	10.1	−104.9	27.83
S2 C1	15.8	−276.2	−149.3
S2 C2	18.6	−79	35.8
S2 C2 TCC	13.2	−57.18	70.68
S3 C1	15.5	−404.3	−210.3
S3 C2	12	−147.9	10.4
S3 C2 TCC	11	−121.3	52.8
S4	17.7	−64.8	−34.8
S5	19.3	−98.5	−48.1
S6 C1	21.1	−520	−243.15
S6 C2	19.2	−162.8	139.9
S6 C2 TCC	14.8	−156.5	146.8

Where Si = Scenario i (i = 1 to 6); Cj = Case j (j = 1 to 2).

- CO_2 Emission Reduction Potential

Using an emission factor of 2680 tCO_2eq per megaliter (ML) of diesel consumed (Raglan data), the avoided CO_2 emissions for each scenario were calculated based on the diesel savings presented in Table 24. Annual and cumulative avoided emissions (over a 15-year project lifetime) are summarized in Table 26.

These results demonstrate that while full decarbonization scenarios (e.g., Scenario 6) maximize avoided CO_2 emissions, they remain economically prohibitive under current cost assumptions. By contrast, Scenario 2 Case 2 (SOFC + TCC) provides a strong compromise, achieving ~61,000 tCO_2eq avoided annually (~0.91 Mt over the project lifetime) with moderate costs and an improved ROI.

Table 26. Estimated avoided CO_2 emissions compared to baseline diesel system.

Scenario	Diesel Savings (ML/Year)	CO_2 Avoided (t/Year)	CO_2 Avoided (Mt Over 15 Years)
Scenario 1 Case 2	22.0	~59,000	~0.89
Scenario 2 Case 2 (SOFC + TCC)	22.8	~61,000	~0.91
Scenario 3 Case 2	27.8	~74,500	~1.12
Scenario 4 Case 2	39.0	~104,500	~1.57
Scenario 5 Case 2	48.0	~129,000	~1.94
Scenario 6 Case 1	53.3	~143,000	~2.15

- Qualitative Multi-Criteria Assessment

A qualitative multi-criteria decision framework was applied to contextualize the scenarios. The criteria considered include:

1. Technical feasibility—reliability under Arctic conditions, proven integration.
2. Environmental performance—diesel reduction and avoided CO_2.
3. Economic viability—CAPEX, ROI, NPV.
4. System flexibility—capacity to valorize excess electricity and scale to transport/heating.

Under this framework, Scenario 2, Case 2, with SOFC + TCC, emerges as the most balanced option, combining technical feasibility, economic viability, and significant CO_2 reductions. In contrast, Scenario 6 achieves the highest emissions savings but scores poorly in terms of economic viability, requiring significant cost reductions and policy support to become feasible. Future work should include refined assumptions regarding fuel prices, inflation, subsidies, and integration of sector-coupling technologies (e.g., waste heat recovery, demand-side management) to optimize both energy and financial outcomes. Additionally, a comprehensive Multi-Criteria Decision Analysis (MCDA) with explicit weighting of criteria necessitates further collaboration with stakeholders to more accurately capture decision-maker priorities and contextual factors.

5.3. Sensitivity Analysis

Hydrogen technologies are evolving rapidly, making cost estimation uncertain due to both technological progress and the limited availability of critical materials. The sensitivity analysis presented here focuses on Case 2 of Scenario 3 (total decarbonization), since this configuration exhibits the highest share of hydrogen technologies in both CAPEX and OPEX.

5.3.1. Electrolyzer

For this study, electrolyzer costs were taken from IRENA's volume-based estimates [56]. In the baseline configuration, electrolyzers account for less than 7% of total project CAPEX and OPEX. To assess their influence, several simulations were performed with varying electrolyzer costs (Figure 5).

The results indicate that even if electrolyzer costs increase by 50%, the overall project CAPEX rises by only 3.4%. The impact on OPEX is somewhat higher: a 40% increase in electrolyzer costs raises the system's total OPEX by just over 4%. These results suggest that while electrolyzers are technologically central, their cost evolution has only a modest effect on the overall economics of the decarbonization scenarios.

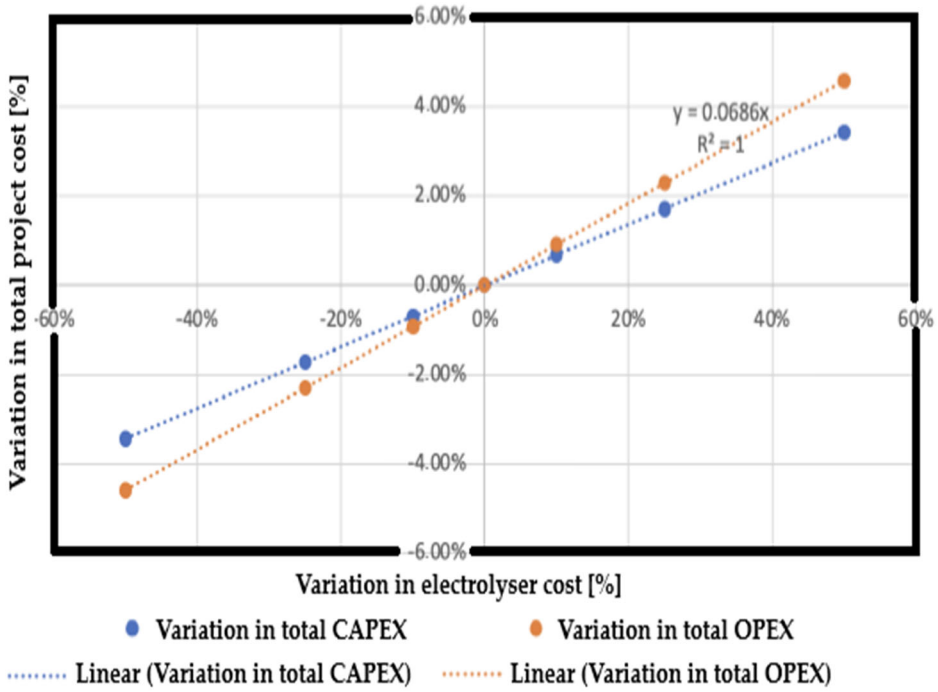

Figure 5. Variation in CAPEX and OPEX costs for the project based on electrolyzer costs.

5.3.2. Hydrogen Storage

In this study, hydrogen is assumed to be stored in sealed, reinforced tanks designed to meet all safety standards. Reliable cost data for this technology remain scarce, and estimates are primarily derived from literature values. Actual costs at Raglan could be higher, as additional protective measures (e.g., insulation, shelters, or hangars) may be required to withstand extreme Arctic conditions. To capture this uncertainty, a sensitivity analysis was performed by varying storage costs between −40% and +40% (Figure 6).

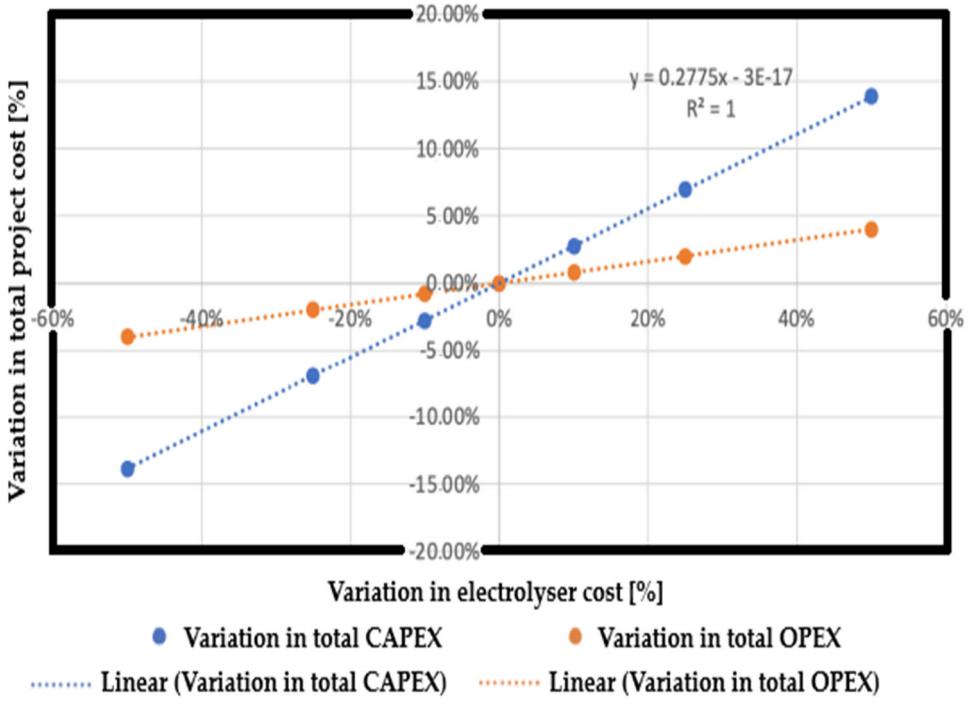

Figure 6. Variation in total project cost based on the cost of the hydrogen storage tank.

The results show that, unlike electrolyzers, hydrogen storage costs have a more substantial influence on project economics. A ±50% variation in tank costs leads to a change of approximately 14% in total project CAPEX and 4% in total OPEX. This confirms that storage infrastructure is one of the key economic drivers of hydrogen-based systems in Arctic contexts.

To reduce costs, alternative large-scale storage options such as underground hydrogen storage in salt caverns or depleted gas reservoirs may be considered. In the specific case of Raglan, repurposing existing mining galleries could be a promising approach, provided safety and permeability conditions are met. The effects of storing hydrogen in permafrost environments would need to be carefully assessed; if unsuitable, the galleries could potentially be salinized to enable safe and cost-effective storage. Such solutions could substantially reduce overall storage costs and improve the long-term feasibility of hydrogen integration at Raglan Mine.

5.3.3. Fuel Cells

Fuel cell costs remain particularly difficult to estimate due to the limited availability of reliable data. This uncertainty is even greater for SOFCs, which can provide both electricity and heat, but are still in the early stages of commercialization. To assess the robustness of the results, a sensitivity analysis was performed with fuel cell costs varied between −50% and +50% (Figure 7).

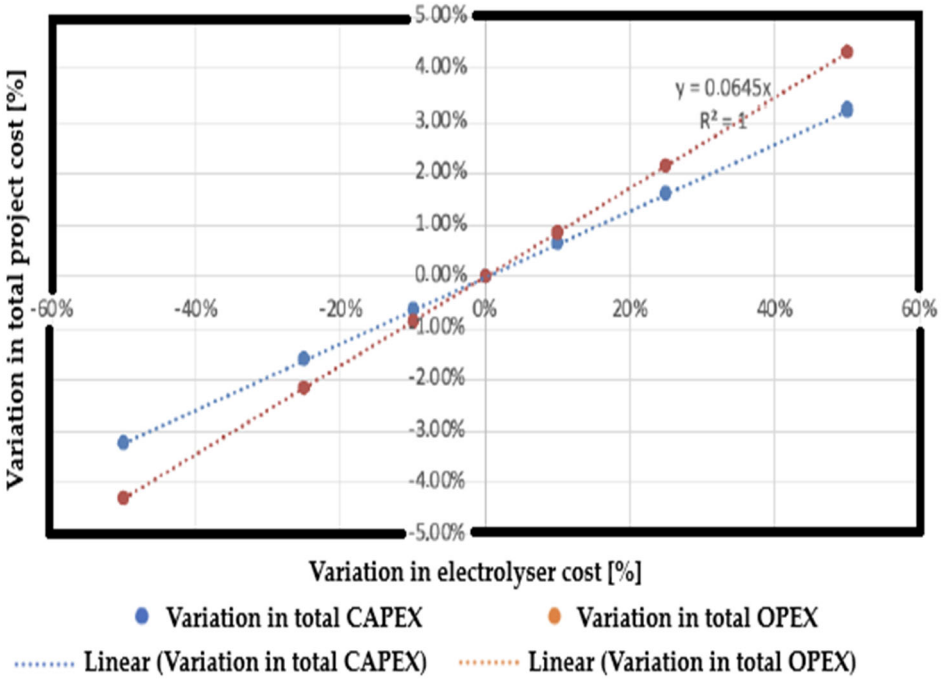

Figure 7. Variation in total project cost based on fuel cell cost.

The simulations show that, similar to electrolyzers, variations in OPEX have a more substantial relative impact than those in CAPEX. Nevertheless, even when fuel cell costs are increased or decreased by 50%, the total project cost changes by less than 5%. This suggests that, although fuel cell technology assumptions introduce some uncertainty, they do not significantly impact the overall economic conclusions of the study.

5.4. Challenges of Exploiting Renewable Energy in the Arctic

The integration of renewable energy sources in Arctic environments faces numerous challenges and uncertainties, including extreme weather conditions, intermittency caused

by both low and excessive wind speeds, turbine icing, and, in some cases, river freezing (e.g., the STEP project [51]). In northern Quebec, wind turbine operation is particularly affected by ice accumulation on blades, which reduces power output and increases mechanical loads on rotors. Under severe conditions, turbines may need to be shut down entirely. Although autonomous de-icing systems exist and can limit the need for manual intervention, they add complexity and cost to system operation.

Future studies will further examine these issues by analyzing the quality and reliability of energy production under Arctic conditions, the impacts of intermittency and climate change, and the resilience of renewable technologies. In addition, risks associated with long-term operation, such as persistent ice formation, accelerated material wear, and restricted access for maintenance, must be considered when assessing the feasibility and durability of renewable energy infrastructure in such environments.

6. Conclusions

The growing awareness of global warming, the volatility of oil prices, and the expected rise in carbon pricing have motivated Raglan Mine to actively pursue pathways for decarbonization. Reducing diesel consumption and, consequently, GHG emissions offers both environmental and economic benefits in this isolated Arctic mining context, where fuel supply is logistically complex and costly. This study conducted a comprehensive techno-economic assessment of progressive decarbonization scenarios for Raglan, based on wind generation coupled with hydrogen production and storage. Using operational data from 2021 and HOMER-based simulations, the analysis considered the mine's primary energy uses, including electricity, heat, and hydrogen demand for equipment and transportation, under six staged scenarios ranging from partial decarbonization of the 25 kV network to full site-wide electrification. The results confirm that wind–hydrogen hybrid systems could technically enable the complete decarbonization of Raglan Mine. However, current hydrogen technologies remain economically constrained, as high CAPEX for electrolyzers, fuel cells, and storage tanks yield negative discounted NPVs under current cost conditions. Among the options analyzed, SOFCs show particular promise due to their cogeneration capability, although their commercialization is still in its early stages. The study also demonstrates that valorizing surplus renewable electricity is essential for improving project feasibility. In particular, thermal integration through TCCs reduced diesel heating demand by ~40% and shortened ROI. Additional valorization pathways, including electrification of auxiliary fleets and the future potential for hydrogen or ammonia export, could further enhance system viability.

At the same time, several critical challenges remain. Dynamic aspects of power quality, such as frequency control, voltage stability, and system inertia, were beyond the scope of this analysis but are crucial for reliable operation under Arctic conditions and will be addressed in future work. Further studies should also refine heating strategies, assess wind resource variability through probabilistic approaches, and evaluate long-term climate impacts on system performance. Notably, storage costs emerged as the most influential economic parameter, with sensitivity results showing a variation of up to 14% in total CAPEX for $\pm$50% changes in storage costs. Innovative solutions such as geological storage in permafrost or repurposing of mining galleries could significantly reduce costs and merit further investigation.

This study confirms that the integration of wind power with hydrogen technologies offers a technically viable pathway for the decarbonization of Raglan Mine. The results highlight clear trade-offs across scenarios. While Scenario 6 (complete decarbonization) achieves the most significant environmental impact, avoiding up to 143,000 tCO_2eq

annually (~2.15 Mt over 15 years), it remains economically unfeasible under current cost structures.

In contrast, Scenario 2 Case 2 (SOFC + TCC integration) emerges as the most influential and immediately viable pathway. It achieves substantial reductions—approximately 61,000 tCO_2eq annually (~0.91 Mt over 15 years)—while offering a more favorable balance of technical feasibility, economic performance, and system flexibility.

A qualitative multi-criteria assessment reinforces this conclusion: Scenario 2 Case 2 achieves the best overall trade-off, while Scenario 6 remains an aspirational target contingent on cost reductions, technological advances, and policy support. These findings underscore that near-term decarbonization can be achieved through incremental yet impactful steps, with complete decarbonization possible in the longer term as technologies mature. Future research will extend this framework by incorporating stakeholder input for criteria weighting, enabling a more robust decision-support tool tailored to Arctic mining contexts.

In conclusion, this study provides one of the first detailed techno-economic evaluations of a wind–hydrogen system applied to a large industrial Arctic mine. It demonstrates that while complete decarbonization of Raglan Mine is technically feasible, achieving economic viability will depend on substantial cost reductions, supportive policy measures such as carbon pricing or subsidies, and advances in storage technologies. Continued research and innovation in these areas will be key to transforming Arctic microgrids into resilient, low-carbon energy systems.

Author Contributions: Conceptualization, H.A. and D.R.R.; methodology, H.A., D.R.R., B.-J.R.M.B. and A.I.; software, H.A.; validation, D.R.R. and B.-J.R.M.B.; formal analysis, H.A., D.R.R., B.-J.R.M.B. and A.I.; investigation, H.A. and D.R.R.; resources, D.R.R.; data curation, H.A.; writing—original draft preparation, H.A., D.R.R. and B.-J.R.M.B.; writing—review and editing, D.R.R. and A.I.; visualization, H.A. and B.-J.R.M.B.; supervision, D.R.R.; project administration, D.R.R.; funding acquisition, D.R.R. All authors have read and agreed to the published version of the manuscript.

Funding: The authors thank Glencore and Hatch industrial partners for their support during this project. They also acknowledge the FRQ-NT's financial support via grants 322720, 340327, and 364164, as well as NSERC's grant RGPIN-2025-04831 and the Michel Trottier private donation to the T3E research group.

Data Availability Statement: The original contributions presented in this study are included in the article. Further inquiries can be directed to the corresponding author.

Acknowledgments: The authors acknowledge the data and information from the industrial partners Glencore and Hatch. The authors did not use generative AI technologies while preparing this work. The authors utilized AI-assisted technologies, including Grammarly (www.grammarly.com) and Antidote (www.antidote.info), to enhance the formulation and eliminate grammatical errors. After using this tool/service, the author(s) reviewed and edited the content as needed and take(s) full responsibility for the publication's content.

Conflicts of Interest: The authors declare no conflicts of interest.

Abbreviations

Abbreviation	Definition
BESS	Battery Energy Storage System
CAPEX	Capital Expenditure
CCS	Carbon Capture and Storage
CO_2	Carbon Dioxide
DGUs	Diesel Generator Units
DOE	U.S. Department of Energy

EMD	Electro-Motive Diesel (type of generator used at Raglan)
FC	Fuel Cell
GHG	Greenhouse Gas
Gt	Gigatonne
H_2	Hydrogen
HOMER	Hybrid Optimization Model for Electric Renewables (software)
IEA	International Energy Agency
IRENA	International Renewable Energy Agency
kWh	Kilowatt-hour
LCOE	Levelized Cost of Energy
LCOH	Levelized Cost of Hydrogen
LCOS	Levelized Cost of Storage
LHV	Lower Heating Value
ML	Million Liters
MW	Megawatt
MWh	Megawatt-hour
NPV	Net Present Value
O&M	Operations and Maintenance
OPEX	Operating Expenditure
PEM	Proton Exchange Membrane
PEMFC	Proton Exchange Membrane Fuel Cell
PHSS	Pumped Hydro Storage System
PV	Photovoltaic
ROI	Return on Investment
SMR	Steam Methane Reforming
SOFC	Solid Oxide Fuel Cell
TCC	Thermal Charge Controller
tCO_2eq	Tons of CO_2 Equivalent
WT	Wind Turbine

Appendix A

Table A1. Main equations used in this model.

Equation	Variable	Observation	Definition of Terms
$LCOE\left[\frac{\$}{kWh}\right] = \frac{\sum_{t=1}^{T} \frac{CAPEX_t[\$]+OPEX_t[\$]}{(1+i[\%])^t}}{\sum_{t=1}^{T} \frac{Q_t[kWh]}{(1+i[\%])^t}}$	*LCOE*	Equation taken from the IRENA [56] report "Renewable power generation costs 2021"	$CAPEX_t$: investment expenditure for year t $OPEX_t$: operating and maintenance and fuel expenses during year t Q_t: electricity production during year t i: discount rate T: system lifetime
$LCOS\left[\frac{\$}{kWh}\right] = \frac{A+B}{\sum_{t=1}^{T} \frac{Elec_{discharged}[kWh]}{(1+i[\%])^t}}$ Where $A = CAPEX_t[\$] + \sum_{t=1}^{T} \frac{OPEX_t[\$]}{(1+i[\%])^t} + \sum_{t=1}^{T} \frac{Charging\ cost[\$]}{(1+i[\%])^t}$ $B = \frac{End-of-life\ cost[\$]}{(1+i[\%])^{T+1}}$	LCOS	The LCOS equation is taken from the work of Schmidt et al. [57].	*Charging cost*: cost of electricity (or more broadly of energy) needed to power the system. $End-of-life\ cost$: either the dismantling cost or the value of the installation at the end of the system's life (salvage value) $Elec_{discharged}$: annual amount of electricity discharged by the system
$Q = m \times Cp \times \Delta T$	Amount of heat	The specific heat capacity of the exhaust gases is taken as 1066 $J \cdot kg^{-1} \cdot K^{-1}$	m: mass of exhaust gases Cp: The specific heat capacity of the exhaust gases ΔT: Temperature variation
$OPEX\left[\frac{\$}{MWh}\right] = \frac{1000}{Fc \times 8760} \times OPEX\left[\frac{\$}{kW.an}\right]$	OPEX	LCOE corresponds to the addition of CAPEX and OPEX.	Fc: load factor

Table A1. *Cont.*

Equation	Variable	Observation	Definition of Terms
$CAPEX\left[\frac{\$}{MWh}\right] = \frac{1000}{Fc \times 8760 \times D} \times CAPEX\left[\frac{\$}{kW}\right]$	CAPEX	LCOE corresponds to the addition of CAPEX and OPEX.	Fc: load factor D: project lifespan
$PV = \frac{A}{t-i} * \left(1 - \frac{(1+i)^{N-1}}{(1+t)^N}\right)$	Present value (PV)	Each investor is free to choose their own inflation and discount rates to judge the economic feasibility of their projects.	$\begin{cases} N: \text{the number of years separating the expenditure from the expenditure from the discount date} \\ i: \text{the inflation rate} \\ t: \text{the discount rate} \end{cases}$ PV: actual value A: the savings made over a year.
$NPV = \sum_{k=1}^{N} \sum_{j=1}^{M} PV_{j,k} - I_{init} + V_{res}$	NPV		I_{init}: initial investment V_{res}: the discounted residual value is the resale price of the system at the end.
$E_{recovH}[MWh] = 0.39 * E_0$	Heat recovered		E_0: initial energy E_{recovH}: energy recovered in the form of heat
$E_0[MWh] = \frac{1}{\eta_{EMD}} \times P_{elecRec}$	Initial energy		η_{EMD}: EMD electrical efficiency $P_{elecRec}$: Recovered electrical power

References

1. United Nations et Framework Convention on Climate Change (UNFCCC). *Report of the Conference of the Parties on its Twenty-First Session, Held in Paris from 30 November to 13 December 2015*; Part one: Proceedings, Paris, FCCC/CP/2015/10; UNFCCC: Bonn, Germany, 2016.
2. Jahangiri, Z.; Hendriks, R.; McPherson, M. A machine learning approach to analysis of Canadian provincial power system decarbonization. *Energy Rep.* **2024**, *11*, 4849–4861. [CrossRef]
3. Government of Canada. Canada's Official Greenhouse Gas Inventory. Annex 13—Electricity in Canada. Available online: https://open.canada.ca/data/en/dataset/779c7bcf-4982-47eb-af1b-a33618a05e5b (accessed on 9 January 2025).
4. Government of Canada. Canadian Net-Zero Emissions Accountability Act. Available online: https://www.canada.ca/en/services/environment/weather/climatechange/climate-plan/net-zero-emissions-2050/canadian-net-zero-emissions-accountability-act.html (accessed on 9 January 2025).
5. Saffari, M.; McPherson, M. Assessment of Canada's electricity system potential for variable renewable energy integration. *Energy* **2022**, *250*, 123757. [CrossRef]
6. Serra, L. Barrières à l'Implantation de Projets d'Énergie Renouvelable dans les Communautés Hors Réseau des Régions Nordiques Canadiennes. Université de Sherbrooke. 2011. Available online: https://savoirs.usherbrooke.ca/handle/11143/7458 (accessed on 15 June 2025).
7. Nieminen, G.S.; Laitinen, E. Understanding local opposition to renewable energy projects in the Nordic countries: A systematic literature review. *Energy Res. Soc. Sci.* **2025**, *122*, 103995. [CrossRef]
8. Satymov, R.; Bogdanov, D.; Galimova, T.; Breyer, C. Energy and industry transition to carbon-neutrality in Nordic conditions via local renewable sources, electrification, sector coupling, and power-to-X. *Energy* **2025**, *319*, 134888. [CrossRef]
9. Chen, S. Measuring regional variations and analyzing determinants for global renewable energy. *Renew. Energy* **2025**, *244*, 122644. [CrossRef]
10. Miremadi, I.; Saboohi, Y.; Arasti, M. The influence of public R&D and knowledge spillovers on the development of renewable energy sources: The case of the Nordic countries. *Technol. Forecast. Soc. Change* **2019**, *146*, 450–463. [CrossRef]
11. Arriaga, M.; Canizares, C.A.; Kazerani, M. Renewable Energy Alternatives for Remote Communities in Northern Ontario, Canada. *IEEE Trans. Sustain. Energy* **2013**, *4*, 661–670. [CrossRef]
12. Arriaga, M.; Canizares, C.A.; Kazerani, M. Northern Lights: Access to Electricity in Canada's Northern and Remote Communities. *IEEE Power Energy Mag.* **2014**, *12*, 50–59. [CrossRef]
13. Bridier, L.; Hernández-Torres, D.; David, M.; Lauret, P. A heuristic approach for optimal sizing of ESS coupled with intermittent renewable sources systems. *Renew. Energy* **2016**, *91*, 155–165. [CrossRef]
14. El-Fouly, T. Canada's First Isolated Smart Microgrid: Hartley Bay, BC. 2020. Available online: https://ressources-naturelles.canada.ca/carte-outils-publications/publications/premier-micro-reseau-intelligent-isole-canada-hartley-bay-c-b (accessed on 15 June 2025).
15. BBA. Les Défis d'Intégrer des Sources d'Énergie Renouvelable sur les Réseaux Électriques Autonomes. 2019. Available online: https://www.bba.ca/ca-fr/publications/dÃl'fis-dintegrer-source-energie-renouvelable-sur-les-reseaux-electriques-autonomes (accessed on 15 June 2025).
16. Colbertaldo, P.; Agustin, S.B.; Campanari, S.; Brouwer, J. Impact of hydrogen energy storage on California electric power system: Towards 100% renewable electricity. *Int. J. Hydrogen Energy* **2019**, *44*, 9558–9576. [CrossRef]

17. McIlwaine, N.; Foley, A.M.; Morrow, D.J.; Al Kez, D.; Zhang, C.; Lu, X.; Best, R.J. A state-of-the-art techno-economic review of distributed and embedded energy storage for energy systems. *Energy* **2021**, *229*, 120461. [CrossRef]
18. Multon, B.; Robin, G.; Erambert, E.; Ahmed, H.B. Stockage de L'énergie Dans les Applications Stationnaires. In Proceedings of the Colloque Energie Électrique: Besoins, Enjeux, Technologies et Applications, Belfort, France, 18 June 2004; pp. 64–77. Available online: https://hal.science/hal-00676113v1/document (accessed on 15 June 2025).
19. Deusen, Z.L.D. Role of energy storage technologies in enhancing grid stability and reducing fossil fuel dependency. *Int. J. Hydrogen Energy* **2025**, *102*, 1055–1074. [CrossRef]
20. Anas, M.; Ram, S.; Thekkepat, K.; Lee, Y.-S.; Bhattacharjee, S.; Lee, S.-C. Influence of oxidation on hydrogen storage properties in titanium-based materials. *Int. J. Hydrogen Energy* **2025**, *105*, 148–155. [CrossRef]
21. Yan, H.; Yu, Y.; Liu, Z.; Xue, B.; Zhou, C.; Huang, K.; Liu, L.; Li, X.; Yu, J. The carbon-clean electricity-lightweight material nexus of the CCS technology benefits for the hydrogen fuel cell buses. *Int. J. Hydrogen Energy* **2025**, *99*, 221–231. [CrossRef]
22. Nagem, N.A.; Ebeed, M.; Alqahtani, D.; Jurado, F.; Khan, N.H.; Hafez, W.A. Optimal design and three-level stochastic energy management for an interconnected microgrid with hydrogen production and storage for fuel cell electric vehicle refueling stations. *Int. J. Hydrogen Energy* **2024**, *87*, 574–587. [CrossRef]
23. Taiwo, G.O.; Tomomewo, O.S.; Oni, B.A. A comprehensive review of underground hydrogen storage: Insight into geological sites (mechanisms), economics, barriers, and future outlook. *J. Energy Storage* **2024**, *90*, 111844. [CrossRef]
24. Egermann, P.; Jeannin, L.; Perreaux, M.; Seyfert, F. Optimizing the design and use of underground hydrogen storage facilities with a Linear Programming approach. *Int. J. Hydrogen Energy* **2025**, *99*, 1092–1099. [CrossRef]
25. Oni, B.A.; Bade, S.O.; Sanni, S.E.; Orodu, O.D. Underground hydrogen storage in salt caverns: Recent advances, modeling approaches, barriers, and future outlook. *J. Energy Storage* **2025**, *107*, 114951. [CrossRef]
26. Qian, K.; Li, Y.; Lou, Y.; Wei, T.; Yan, X.; Kobayashi, H.; Qi, D.; Tan, M.; Li, R. Gold-decorated Pt bimetallic nanoparticles on sulfur vacancy-rich MoS2 for aqueous phase reforming of methanol into hydrogen at low temperature and atmospheric pressure. *Appl. Catal. A: Gen.* **2025**, *693*, 120137. [CrossRef]
27. Tabu, B.; Veng, V.; Morgan, H.; Das, S.K.; Brack, E.; Alexander, T.; Mack, J.H.; Wong, H.-W.; Trelles, J.P. Hydrogen from cellulose and low-density polyethylene via atmospheric pressure nonthermal plasma. *Int. J. Hydrogen Energy* **2024**, *49*, 745–763. [CrossRef]
28. Fan, L.; Tu, Z.; Chan, S.H. Recent development of hydrogen and fuel cell technologies: A review. *Energy Rep.* **2021**, *7*, 8421–8446. [CrossRef]
29. Kadirgama, K.; Samylingam, L.; Aslfattahi, N.; Kiai, M.S.; Kok, C.K.; Yusaf, T. Advancements and challenges in numerical analysis of hydrogen energy storage methods: Techniques, applications, and future direction. *Int. J. Hydrogen Energy* **2025**, *125*, 67–85. [CrossRef]
30. Zavala, V.R.; Pereira, I.B.; Vieira, R.d.S.; Aires, F.I.d.S.; Dari, D.N.; Félix, J.H.d.S.; de Lima, R.K.C.; dos Santos, J.C.S. Challenges and innovations in green hydrogen storage technologies. *Int. J. Hydrogen Energy* **2025**, *113*, 322–339. [CrossRef]
31. Hua, Z.; Gao, W.; Chi, S.; Wang, X.; Zheng, J. Development status and challenges of high-pressure gaseous hydrogen storage vessels and cylinders in China. *Renew. Sustain. Energy Rev.* **2025**, *214*, 115567. [CrossRef]
32. Mehrizi, M.Z.; Abdi, J.; Rezakazemi, M.; Salehi, E. A review on recent advances in hollow spheres for hydrogen storage. *Int. J. Hydrogen Energy* **2020**, *45*, 17583–17604. [CrossRef]
33. Zhang, F.; Zhao, P.; Niu, M.; Maddy, J. The survey of key technologies in hydrogen energy storage. *Int. J. Hydrogen Energy* **2016**, *41*, 14535–14552. [CrossRef]
34. Wang, H.; Jie, Y.; Zhou, D.; Ma, X. Underground hydrogen storage in depleted gas reservoirs with hydraulic fractures: Numerical modeling and simulation. *J. Energy Storage* **2024**, *97*, 112777. [CrossRef]
35. Wallace, R.L.; Cai, Z.; Zhang, H.; Guo, C. Numerical investigations into the comparison of hydrogen and gas mixtures storage within salt caverns. *Energy* **2024**, *311*, 133369. [CrossRef]
36. Ahluwalia, D.D.P.R.K. Bulk storage of hydrogen. *Int. J. Hydrogen Energy* **2021**, *46*, 34527–34541. [CrossRef]
37. Abe, J.O.; Popoola, A.P.I.; Ajenifuja, E.; Popoola, O.M. Hydrogen energy, economy and storage: Review and recommendation. *Int. J. Hydrogen Energy* **2019**, *44*, 15072–15086. [CrossRef]
38. Zhang, Y.; Jia, Z.; Yuan, Z.; Yang, T.; Qi, Y.; Zhao, D. Development and Application of Hydrogen Storage. *J. Iron Steel Res. Int.* **2015**, *22*, 757–770. [CrossRef]
39. Mateti, S.; Zhang, C.; Du, A.; Periasamy, S.; Chen, Y.I. Superb storage and energy saving separation of hydrocarbon gases in boron nitride nanosheets via a mechanochemical process. *Mater. Today* **2022**, *57*, 26–34. [CrossRef]
40. Yao, W.; Niu, F.; Wu, Z.; Gao, S.; Huang, Y. Reversible conversion between bicarbonate and formate in solid state "storage ball" for chemical hydrogen storage. *Int. J. Hydrogen Energy* **2025**, *122*, 229–234. [CrossRef]
41. Du, Y.-L.; Sun, Z.Y.; Fu, B.; Huang, Q. Unleashing the power of hydrogen: Challenges and solutions in solid-state storage. *Int. J. Hydrogen Energy* **2025**, S0360319925010341. [CrossRef]

42. Tan, H.; Shao, Z.; Wang, Q.; Lin, Z.; Li, Z.; Weng, H.; Mohamed, M.A. A coordinated planning method of hydrogen refueling stations and distribution network considering gas-solid two-phase hydrogen storage mode. *Int. J. Hydrogen Energy* **2025**, *100*, 1561–1573. [CrossRef]
43. International Renewable Energy Agency (IRENA). *Green Hydrogen Cost Reduction: Scaling up Electrolysers to Meet the 1.5 °C Climate Goal*; IRENA: Abu Dhabi, United Arab Emirates, 2020; Available online: https://www.irena.org/-/media/Files/IRENA/Agency/Publication/2020/Dec/IRENA_Green_hydrogen_cost_2020.pdf (accessed on 15 June 2025).
44. I.E. Agency. Global Hydrogen Review 2024. International Energy Agency. 2024. Available online: https://www.iea.org/reports/global-hydrogen-review-2024 (accessed on 15 September 2025).
45. I.E. Agency. Global Hydrogen Review 2025. International Energy Agency. 2025. Available online: https://www.iea.org/reports/global-hydrogen-review-2025 (accessed on 15 September 2025).
46. I.E. Agency. Towards Hydrogen Definitions Based on Their Emissions Intensity. International Energy Agency. 2023. Available online: https://www.iea.org/reports/towards-hydrogen-definitions-based-on-their-emissions-intensity (accessed on 15 September 2025).
47. U.S.D. of Energy. Hydrogen Shot: A Bold Decadal Vision for Reducing the Cost of Clean Hydrogen. DOE. 2021. Available online: https://www.energy.gov/eere/fuelcells/hydrogen-shot (accessed on 15 September 2025).
48. da Silva, F.T.F.; Lopes, M.S.G.; Asano, L.M.; Angelkorte, G.; Costa, A.K.B.; Szklo, A.; Schaeffer, R.; Coutinho, P. Integrated systems for the production of food, energy and materials as a sustainable strategy for decarbonization and land use: The case of sugarcane in Brazil. *Biomass Bioenergy* **2024**, *190*, 107387. [CrossRef]
49. Du, Y.; Shen, X.; Kammen, D.M.; Hong, C.; Nie, J.; Zheng, B.; Yao, S. A generation and transmission expansion planning model for the electricity market with decarbonization policies. *Adv. Appl. Energy* **2024**, *13*, 100162. [CrossRef]
50. Balaban, G.; Dumbrava, V.; Lazaroiu, A.C.; Kalogirou, S. Analysis of urban network operation in presence of renewable sources for decarbonization of energy system. *Renew. Energy* **2024**, *230*, 120870. [CrossRef]
51. Dongsheng, C.; Ndifor, E.Z.; Olayinka, A.-O.T.; Ukwuoma, C.C.; Shefik, A.; Hu, Y.; Bamisile, O.; Dagbasi, M.; Ozsahin, D.U.; Adun, H. An EnergyPlan analysis of electricity decarbonization in the CEMAC region. *Energy Strategy Rev.* **2024**, *56*, 101548. [CrossRef]
52. Obiora, S.C.; Bamisile, O.; Hu, Y.; Ozsahin, D.U.; Adun, H. Assessing the decarbonization of electricity generation in major emitting countries by 2030 and 2050: Transition to a high share renewable energy mix. *Heliyon* **2024**, *10*, e28770. [CrossRef]
53. Kumar, T.R.; Beiron, J.; Marthala, V.R.R.; Pettersson, L.; Harvey, S.; Thunman, H. Combining exergy-pinch and techno-economic analyses for identifying feasible decarbonization opportunities in carbon-intensive process industry: Case study of a propylene production technology. *Energy Convers. Manag. X* **2025**, *25*, 100853. [CrossRef]
54. Robert, A.; Bisulandu, B.-J.R.M.; Ilinca, A.; Rousse, D.R. Hybrid Wind–Redox Flow Battery System for Decarbonizing Off-Grid Mining Operations. *Appl. Sci.* **2025**, *15*, 7147. [CrossRef]
55. Tardy, A.; Rousse, D.R.; Bisulandu, B.-J.R.M.; Ilinca, A. Enhancing Energy Sustainability in Remote Mining Operations Through Wind and Pumped-Hydro Storage; Application to Raglan Mine, Canada. *Energies* **2025**, *18*, 2184. [CrossRef]
56. International Renewable Energy Agency (IRENA). *Renewable Power Generation Costs in 2021*; IRENA: Abu Dhabi, United Arab Emirates, 2022; Available online: https://www.irena.org/publications/2022/Jul/Renewable-Power-Generation-Costs-in-2021 (accessed on 15 June 2025).
57. Schmidt, O.; Melchior, S.; Hawkes, A.; Staffell, I. Projecting the Future Levelized Cost of Electricity Storage Technologies. *Joule* **2019**, *3*, 81–100. [CrossRef]